NASA TECHNICAL NOTE

NASA TN D-8413

EXPERIMENTAL AND ANALYTICAL DYNAMIC FLOW CHARACTERISTICS OF AN AXIAL-FLOW FAN FROM AN AIR CUSHION LANDING SYSTEM MODEL

William C. Thompson, Ashok B. Boghani, and Trafford J. W. Leland

Langley Research Center
Hampton, Va. 23665

NATIONAL AERONAUTICS AND SPACE ADMINISTRATION • WASHINGTON, D. C. • JULY 1977

1. Report No.	2. Government Accession No.	3. Recipient's Catalog No.
NASA TN D-8413		

4. Title and Subtitle
EXPERIMENTAL AND ANALYTICAL DYNAMIC FLOW CHARACTERISTICS OF AN AXIAL-FLOW FAN FROM AN AIR CUSHION LANDING SYSTEM MODEL

5. Report Date
July 1977

6. Performing Organization Code

7. Author(s)
William C. Thompson, Ashok B. Boghani, and Trafford J. W. Leland

8. Performing Organization Report No.
L-11154

10. Work Unit No.
505-08-31-01

9. Performing Organization Name and Address
NASA Langley Research Center
Hampton, Va 23665

11. Contract or Grant No.

13. Type of Report and Period Covered
Technical Note

12. Sponsoring Agency Name and Address
National Aeronautics and Space Administration
Washington, DC 20546

14. Sponsoring Agency Code

15. Supplementary Notes
William C. Thompson and Trafford J. W. Leland: Langley Research Center.
Ashok B. Boghani: Foster-Miller Associates, Inc., Waltham, Massachusetts.

16. Abstract

An investigation was conducted to compare the steady-state and dynamic flow characteristics of an axial-flow fan which had been used previously as the air supply fan for some model air cushion landing system studies. Steady-state flow characteristics were determined in the standard manner by using differential orifice pressures for the flow regime from free flow to zero flow. In this same regime, a correlative technique was established so that fan inlet and outlet pressures could be used to measure dynamic flow as created by a rotating damper. Dynamic tests at damper frequencies up to 5 Hz showed very different flow characteristics when compared with steady-state flow, particularly with respect to peak pressures and the pressure-flow relationship at fan stall and unstall.

A generalized, rational mathematical fan model was developed based on physical fan parameters and a steady-state flow characteristic. The model showed good correlation with experimental tests at damper frequencies up to 5 Hz.

17. Key Words (Suggested by Author(s))
Axial fan flow
Air cushion landing system
Dynamic flow characteristics

18. Distribution Statement
Unclassified – Unlimited

Subject Category 09

19. Security Classif. (of this report)	20. Security Classif. (of this page)	21. No. of Pages	22. Price*
Unclassified	Unclassified	47	$4.00

*For sale by the National Technical Information Service, Springfield, Virginia 22161

EXPERIMENTAL AND ANALYTICAL DYNAMIC FLOW CHARACTERISTICS OF AN AXIAL-FLOW FAN FROM AN AIR CUSHION LANDING SYSTEM MODEL

William C. Thompson, Ashok B. Boghani,*
and Trafford J. W. Leland
Langley Research Center

SUMMARY

An investigation was conducted to compare the steady-state and dynamic flow characteristics of an axial-flow fan which had been used previously as the air supply fan for some model air cushion landing system studies. Steady-state flow characteristics were determined in the standard manner by using differential orifice pressures for the flow regime from free flow to zero flow. In this same regime, a correlative technique was established so that fan inlet and outlet pressures could be used to measure dynamic flow as created by a rotating damper. Dynamic tests at damper frequencies up to 5 Hz showed very different flow characteristics when compared with steady-state flow, particularly with respect to peak pressures and the pressure-flow relationship at fan stall and unstall.

A generalized, rational mathematical fan model was developed based on physical fan parameters and a steady-state flow characteristic. The model showed good correlation with experimental tests at damper frequencies up to 5 Hz.

INTRODUCTION

The performance of an air cushion landing system (ACLS) for aircraft depends upon an adequate and continuous supply of low pressure air. This low pressure air must often be supplied under widely varying and rapidly changing flow conditions. Thus, the air supply fan and its dynamic flow characteristics form an integral and possibly influential part of any ACLS. During the course of some recent experimental studies of an ACLS model (refs. 1 and 2), concern was expressed regarding the accuracy and validity of the methods used to measure airflow of an axial fan under dynamic conditions, since the interpretation of the measurements depended upon the steady-state pressure-flow characteristics furnished by the fan manufacturer. Therefore, this study was undertaken to provide a better understanding of overall ACLS behavior. During this investigation, the

*Program Manager, Foster-Miller Associates, Inc., Waltham, Massachusetts.

fan was isolated from the rest of the system, and fan flow characteristics were studied in detail over a wide range of changing input and output conditions.

The overall objectives of this study were threefold: (1) to establish a technique for measuring fan flow on the fan itself as an aid to future experimental studies since ACLS model configurations generally preclude the use of standard fan flow measurement techniques; (2) to observe and to compare fan flow behavior under steady-state and dynamic conditions over a frequency range thought to be of significance in ACLS model studies; and (3) to provide an experimental basis for the development of a rational mathematical fan model to refine the analytical ACLS model of reference 3 in which fan flow characteristics were estimated from steady-state data. The approach taken to reach these objectives was to construct a fan test bench in strict accordance with American Society of Mechanical Engineers (ASME) standards (ref. 4) where steady-state flow is computed from measurements of the pressure drop across an orifice. This apparatus would then be used to duplicate, if possible, the characteristic pressure-flow curve provided by the fan manufacturer and to investigate various fan measurement techniques which might prove correlatable with the ASME standard. Once a good confidence level in results was established, testing would then be continued to examine the effects of a restricted fan inlet, the effects of rapidly changing back pressure produced by a rotating damper, and the effects of changes in air volume between the fan and the damper.

This paper presents the results of the experimental investigation of steady-state and dynamic flow characteristics of an axial fan and shows the development of a rational mathematical fan model based on these test results.

SYMBOLS

Values are given in both SI and U.S. Customary Units. The measurements and calculations were made in U.S. Customary Units. Factors relating the two systems are given in reference 5. Unless otherwise noted, all pressures are gage pressures.

A cross-sectional area of flow in fan, m^2 (ft^2)

A_e effective exit area, m^2 (ft^2)

A_i cross-sectional area of ith stream tube, m^2 (ft^2)

A_o orifice area, m^2 (ft^2)

C_e discharge coefficient

C_f capacitance of fan, m^5/N (ft^5/lb)

C_t	lumped duct capacitance, m^5/N (ft^5/lb)
D	flow tube diameter (damper diameter), m (ft)
f	frequency of damper shaft rotation, Hz
I_f	lumped inertia of fluid in fan, Ns^2/m^5 ($lb\ s^2/ft^5$)
I_{fi}	inertance of fluid in ith stream tube, Ns^2/m^5 ($lb\ s^2/ft^5$)
I_t	lumped duct inertance, Ns^2/m^5 ($lb\ s^2/ft^5$)
k	flow coefficient
l	average fan flow path length, m (ft)
l_i	flow path length of ith stream tube, m (ft)
n	polytropic constant
p	average air pressure in fan (absolute pressure), kPa (lb/ft^2)
p_c	fan outlet pressure, kPa (psfg)
p_t	pitot static pressure upstream of damper
p_1	pressure upstream from orifice, kPa (psfg)
p_2	pressure downstream from orifice, kPa (psfg)
Δp	fan static pressure rise
Δp_o	pressure drop across orifice, kPa (lb/ft^2)
Q	steady-state fan flow, m^3/s (cfm)
Q_d	fan outlet flow, m^3/s (cfm)
Q_f	capacitance flow, m^3/s (cfm)

t time, s

V volume of fan cavity, m^3 (ft^3)

β ratio of orifice diameter and pipe diameter

$\nu_0, \ldots, \nu_4$ polynomial coefficients

ρ air mass density (fluid mass density), kg/m^3 ($slug/ft^3$)

APPARATUS AND TEST PROCEDURE

Fan Test Bench

General.- The fan test bench used in this investigation was designed to conform strictly with that portion of the ASME Power Test Code dealing with flow measurement (ref. 4). The code stipulates precisely the required construction and location with respect to the fan of such key components as the flow straightener, the orifice plate, and the pressure taps, each as a function of the diameter of the pipe in which the flow is to be measured. Figure 1 contains a photograph of the overall fan test bench as it finally evolved. Figure 2 shows closeup views of various parts of the apparatus including the fan (fig. 2(a)), the flow straightener (fig. 2(b)), the orifice plate installation (fig. 2(c)), and the flow control damper (fig. 2(d)). A dimensioned schematic of the test bench is shown in figure 3. Details of some of the test bench components are discussed in the following sections.

Flow tube construction.- The flow tube was constructed from clear acrylic plastic seamless tubing of 20.2-cm (8.00-in.) inside diameter with a 0.63-cm (0.25-in.) wall thickness. Several sections were provided, varying in length from approximately 61 to 130 cm (24 to 51 in.), and each section had flanges on both ends which fitted a grooved aluminum external ring clamp (see fig. 2) to provide an airtight seal. The inner surface at each section joint was carefully filled with plasticene to provide a smooth, continuous flow tube. As shown in figure 3, the overall length of the flow tube was approximately 515 cm (202 in.) with all sections assembled. The final or discharge section was a straight tube vented to the atmosphere.

As recommended in reference 4, a flow straightener was located 3 pipe diameters or 60.96 cm (24.00 in.) downstream from the fan. (See fig. 2(b).) The straightener was made from 31 pieces of polyvinyl chloride thin-wall tubing 2.86 cm (1.13 in.) in diameter and 40.64 cm (16 in.) long. The tubes were bonded to each other, and the assembly was attached to the flow tube flange with set screws.

Orifice plate installation.- During the steady-state part of the test, fan flow was determined by measuring the pressure drop across an orifice as outlined in reference 4. The orifice, shown in figure 2(c), was located approximately 280 cm (110 in.) downstream from the fan as shown in figure 3 and was installed in a special holding clamp which assured concentricity of the orifice with the flow tube center line. It was necessary to use four different orifices to cover the entire anticipated range of flow during the test. Each orifice size and appropriate usable flow range (ref. 4) is shown in table I.

Each orifice plate was constructed of clear acrylic plastic sheet 0.63 cm (0.25 in.) thick, and the orifice was carefully turned to have a sharp upstream edge and to be centered in the plate. The orifices were then changed as needed during the steady-state tests and were removed entirely for the dynamic tests.

Flow control damper.- A rotatable aluminum plate was used to control airflow through the flow tube from unrestricted flow (damper fully open) to zero flow (damper fully closed). This plate, shown in figure 2(d), was installed on a through shaft approximately 388 cm (153 in.) downstream from the fan or 108 cm (42.5 in.) downstream from the orifice as shown in figure 3. The plate was approximately 0.25 cm (0.1 in.) thick with smoothed edges to offer minimum resistance to flow when in the 0° (fully open) position, while providing scant daylight clearance between the plate and the inner flow tube wall when in the 90° (fully closed) position. The plate could be positioned manually and could be locked for the steady-state tests. During the dynamic tests, the plate shaft could be rotated at constant velocity by the variable-speed motor and belt drive shown in the background of figure 2(d).

Description of Fan

The fan used in this investigation was an axial-flow fan used in previous ACLS model studies (refs. 1 and 2). This axial-flow fan had an integral 3-phase, 400-Hz electrical motor rated at 11.19 kW (15 hp) with a nominal rotational speed of 11 400 rpm. The fan is shown in the closeup view of figure 2(a) and in the schematic in figure 4 where dimensions are given. As indicated in figure 4, there are 19 stator blades at the inlet end of the fan and 11 stator blades at the outlet end. Between these two sections is the motor-driven 8-blade rotor. An inlet restriction plate, shown in figure 4, was provided so that the inlet gap could be varied from more than 5 cm (2 in.) to less than 0.5 cm (0.2 in.) so that the effects of a restricted fan inlet might be observed.

Instrumentation

The computation of fan flow from the measured pressure drop across an orifice formed a key part of the steady-state tests. The pressure taps, as shown in figure 3, were located as specified in reference 4 with the upstream pressure tap located one pipe

diameter or 20.32 cm (8.00 in.) upstream of the orifice, and the downstream tap located one-half pipe diameter or 10.16 cm (4.00 in.) downstream from the orifice. The pressure taps were drilled in from the outside to be flush with the inner flow tube wall and were connected to strain-gage type of differential pressure transducers with short lengths of thick-wall flexible tubing 0.318 cm (0.125 in.) in diameter to minimize vibration at the transducer. In a similar manner, pressure transducers were connected to taps on the inlet and outlet of the fan itself as shown in figure 2(a) and in the schematic of figure 4. Pressure taps on the fan had been suggested as a possible means of obtaining flow measurements which might be correlatable with the standard ASME orifice measurements. A pitot static pressure probe was tried in several locations as a possible alternate flow measurement technique. Another alternate method tried was to measure fan speed with a small dc generator, but results from early tests were inconclusive, and the method was abandoned. A circular slide wire, attached to the flow control damper shaft as shown in figure 2(d), was used to monitor damper position in both the steady-state and dynamic fan tests. All the above quantities were recorded on a direct-write oscillograph. Additionally, two thermometers were read visually during the test runs; one was located near the fan inlet to measure ambient temperature, and the other was located downstream from the orifice as shown in figure 3.

Test Procedure

Steady-state tests.- The steady-state tests were conducted with the fan test bench in the configuration shown in figures 1 and 3. Normally, each test lasted only 10 to 15 seconds to minimize temperature rise effects on air density. The flow control damper was fixed at the desired position before each test, generally in 10^{o} increments from fully open (0^{o}) to fully closed (90^{o}), and the full travel of damper position was explored, from fully open to fully closed, and back to fully open. This sequence was repeated with each of the four orifices listed in table I in order to cover the entire flow range of the fan. After the basic studies were concluded, the effect of restricted fan inlet was studied by adjusting the inlet restriction plate (fig. 4) in the steps noted in table II.

In all cases during the steady-state tests, fan inlet and outlet pressures were recorded simultaneously with the pressures upstream and downstream from the orifice.

Dynamic tests.- The dynamic tests were generally conducted with the fan test bench configured as shown in figures 1 and 3, except that the orifice was removed. The variable-speed drive motor was employed to rotate the flow control damper shaft (fig. 2(d)) at constant speed. Rotational speeds were selected to produce a damper frequency or a cyclic perturbation in flow varying from 1 to 17 Hz. In this case, a cycle is defined as the movement of the damper from fully open (free flow), through fully closed (zero flow), to fully

open again. Thus, one full shaft rotation produced 2 cycles or perturbations in flow. Damper position was continuously recorded by the circular slide wire shown in figure 2(d).

The effects on dynamic flow characteristics of various degrees of fan inlet restriction were studied in the same manner as for the steady-state tests, using the same inlet gap settings given in table II. Also explored was the effect of reducing the air volume between the fan outlet and the flow control damper. This reduction was accomplished by progressively removing sections of the flow tube. For all test conditions during the dynamic tests, fan inlet and outlet pressures were recorded, and the temperature rise was noted during each test.

EXPERIMENTAL RESULTS

General

A common method of describing the behavior of any fan is to show the airflow output of the fan as a function of the pressure rise across the fan; that is, the difference between ambient pressure and the pressure in the flow tube downstream from the fan. This pressure-flow relationship, referred to as the fan characteristic curve (or simply "characteristic"), is usually obtained under steady-state conditions and is considered an adequate description of fan performance. For an axial-flow fan, the steady-state pressure-flow characteristic curve resembles the curve in sketch (a).

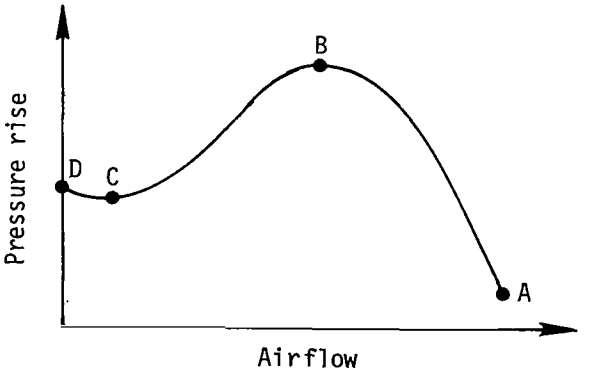

Sketch (a)

The characteristic curve can be divided into three regions: AB, the stable or normal operating region, where A represents the free-flow condition and B represents the stall point of the fan; BC, which occurs if the volume rate of flow is reduced below the stable limit (stall point) and is unstable because of its positive slope; and CD, an extremely unstable region which occurs if volume rate of flow is further reduced to zero (D) or near zero values. It is this characteristic curve and its variations which are derived and discussed in the following sections.

Steady-State Tests

Correlation of pressure measurements.- The most pertinent data acquired during this investigation were in the form of pressure measurements taken at the fan inlet and outlet and upstream and downstream from the orifice. Figure 5 shows the relationship of these measurements for a typical steady-state test with the test bench conditions shown. It should be noted that percent damper opening is computed from damper position based upon projected area. By using the data represented by figure 5, actual airflow through the tube was computed based on the measured orifice differential pressure as follows:

$$Q = kA_o\sqrt{\frac{2\Delta p_o}{\rho}} \tag{1}$$

where

Q steady-state fan flow, m^3/s (ft^3/s, converted to cfm throughout)

k flow coefficient based on Reynolds number (30 000 to 500 000 for these tests) and the diameter ratio β

β $= \frac{\text{Orifice diameter}}{\text{Pipe diameter}}$

A_o orifice area, m^2 (ft^2)

Δp_o measured pressure drop across orifice, $p_1 - p_2$, kPa (lb/ft^2)

p_1 pressure upstream from orifice, kPa (psfg)

p_2 pressure downstream from orifice, kPa (psfg)

ρ air mass density, kg/m^3 ($slug/ft^3$)

Computations of airflow were made for all four orifices used with the results shown in figure 6 where upstream orifice pressure (pressure rise) is plotted as a function of the computed flow. Although measurements were obtained for the entire range of damper position, the usable range of each orifice as given in table I is shown in figure 6. A single line was used to fair the data from each orifice since there appeared to be no significant difference in flow characteristic as the flow passed through the fan stall/fan

unstall region as shown in figure 5. Appropriate segments of these fairings in figure 6 were then used to construct the standard pressure-flow characteristic curve shown in figure 7. Also shown in figure 7 is the flow characteristic curve furnished by the fan manufacturer, and the good agreement gives confidence in the test apparatus and procedures used in the investigation.

With confidence in the apparatus thus established, the next major task was to determine a correlation between true flow measurements based on orifice differential pressure and the fan inlet and outlet pressure measurements which could be obtained during dynamic or model ACLS testing where the use of orifices is impossible. As seen in figure 5, the fan outlet pressure displays the same characteristic shape as the orifice pressure measurements and is nearly equal in magnitude to the upstream orifice pressure. In contrast, the fan inlet pressure shows a quite different characteristic. It is at all times negative and, furthermore, is a single-valued function of damper opening.

This latter feature makes the fan inlet pressure measurement particularly appealing from an experimental model standpoint, and with this in mind, figure 8 was constructed to show the relationship between simultaneous measurements of fan inlet pressure and fan airflow as computed from the orifice differential pressure. As might be expected, the fan inlet pressure is also a single-valued function of, and hence correlatable with, fan airflow. Thus, fan inlet pressure would be useful in experimental model studies. However, from this measurement alone, nothing can be learned regarding the stall point of the fan, and the peak stall pressure and fan flow at the stall are important fan characteristics. As figure 5 shows, the upstream orifice pressure is of the same form and magnitude as the fan outlet pressure; this similarity indicates that the fan outlet pressure might be used as the pressure rise parameter. If measured fan outlet pressure is plotted against airflow as determined from orifice differential pressure, as shown in figure 9, there is excellent agreement with the standard characteristic curve (taken from fig. 7). Thus, a technique for exploring fan flow characteristics is suggested whereby fan outlet pressure describes the pressure rise across the fan and at the same instant, fan inlet pressure provides a measure of fan airflow through the relationship shown in figure 8. In order to use this technique to explore dynamic flow characteristics, the assumption must be made that the instantaneous fan pressure measurements obtained during dynamic tests bear the same relationship to each other and to airflow as for steady-state conditions. One must also assume that no reverse flow occurs. These assumptions were made, and the technique was adopted to display results of low-frequency (less than 10 Hz) dynamic studies discussed in a later section of this paper.

Effects of restricted inlet area.- In many ACLS model studies (ref. 1), a restricted fan inlet was used to reduce rated fan airflow to the quantity desired for a particular system design. In order to explore the effects of such a restriction on fan flow characteristics, the restriction plate described previously was adjusted to reduce the inlet area,

and the results are shown in figure 10. It can be seen from figure 10 that reducing the inlet gap from 2.54 cm (1.0 in.) to 2.03 cm (0.8 in.) had no apparent effect on the flow characteristic, and a further reduction to 1.52 cm (0.6 in.) had only a minor effect. Reductions to 1.02 cm (0.4 in.) and 0.51 cm (0.2 in.), however, radically altered the flow characteristics. A reduction to 0.51 cm (0.2 in.) resulted in a nearly choked flow. Such altered flow characteristics also alter the relationship between fan inlet pressure and airflow as shown in figure 11. It is this relationship between fan inlet pressure and airflow which is used in the discussion of dynamic test results to follow.

Dynamic Tests

Flow characteristics at low damper frequencies.- The dynamic fan flow characteristics in the flow regime of free flow to zero flow as determined from fan inlet and outlet pressures are shown in figure 12 for damper frequencies (or flow perturbation frequencies) up to 5 Hz, a range thought to encompass likely frequencies of ACLS models (ref. 1). As in the steady-state tests, the test duration at each condition was intentionally kept short to minimize temperature rise, and although several cycles were recorded, only one typical cycle at each frequency is shown in figure 12. Also in figure 12 the steady-state flow characteristic (taken from fig. 10) is shown for comparison. It can be seen from figure 12 that in the dynamic case, there is a definite "hysteresis" effect in the sense that the flow follows different paths from free flow to zero flow and back to free flow and that the differences in peak pressure at fan stall and unstall are quite noticeable. This effect becomes more pronounced with increasing frequency as figure 12(d) shows, and it is interesting to note that no such "hysteresis" was observed in the steady-state tests summarized in figure 6. There is also a noticeable phase shift in the sense that the peak pressure occurs at different fan flow values during stall or unstall, and both of these values differ from the steady-state case. These results suggest that a knowledge of dynamic fan characteristics may be important to the design of an air cushion landing system, particularly if the design conditions call for the fan to be operated near the stall point. The "hysteresis" effect could significantly alter system dynamics, particularly during landing impact or obstacle encounter, and could affect the stability of the system.

Effects of restricted inlet area at low frequencies.- It was noted in the steady-state tests that reducing the fan inlet gap (and thus the fan inlet area) resulted in very different pressure-flow characteristics. (See fig. 10.) The effect on dynamic flow characteristics is even more pronounced, as shown in figure 13 for a fan inlet gap of 1.52 cm (0.6 in.), in figure 14 for a fan inlet gap of 1.02 cm (0.4 in.), and in figure 15 for a fan inlet gap of 0.51 cm (0.2 in.). Comparing the results of figure 13 with the unrestricted inlet results of figure 12 illustrates that the same sort of difference exists between steady-state and dynamic flow characteristics with a "hysteresis" loop between stall and unstall and a shift in magnitude and location of peak pressures. These differences become more

obvious with increasing damper frequency, and at 5 Hz, as figure 13(d) shows, the dynamic characteristic bears very little resemblance to the steady-state characteristic. This degrading effect on flow characteristic is further illustrated in figure 14 for an inlet gap of 1.02 cm (0.4 in.) where the steady-state and dynamic characteristics differ quite widely at 2.2 Hz (fig. 14(b)) and again grow progressively worse with increasing frequency. As in figure 13(d), a curious flow path is shown at 5 Hz (fig. 14(d)), and it is difficult to derive a rational explanation for what is actually occurring in this situation. What is obvious is that the steady-state characteristic has less and less meaning with decreasing inlet gap as is illustrated in figure 15 for an inlet gap of 0.51 cm (0.2 in.). This case is no doubt unrealistic from a practical standpoint since inlet restrictions of this degree would not ordinarily be considered, but the results are presented as a "worst case" condition. The results shown in this section reinforce the belief that a knowledge of the dynamic characteristics of the air supply fan is important for ACLS design. The results also show that if flow from a given fan is to be reduced, perhaps some method other than restricting the fan inlet should be considered.

Effect of reduced plenum volume.- All tests discussed thus far were conducted with the fan test bench in the configuration shown in figures 1 and 3. In exploring the effects of reduced plenum volume or "dead volume," various sections of the flow tube were removed to decrease the fan outlet-to-damper distance and thus to decrease the plenum volume. This procedure prohibits any direct comparison with steady-state flow characteristics since the fan outlet-to-orifice distance stipulated in reference 4 is violated. All tests in this section were conducted with the unrestricted fan inlet gap of 2.54 cm (1.00 in.). The flow straightener (fig. 2(b)) was removed for this test series in the interest of uniform test conditions since it would have had to be removed in any case for the smaller plenum volumes required. The first flow tube section to be removed was 0.96 cm (24.00 in.) long; thereby the initial fan outlet-to-damper distance of 387.67 cm (152.63 in.) was reduced to 326.67 cm (128.63 in.) and plenum volume was reduced by 16 percent. The results shown in figure 16 may be compared with the dynamic flow characteristics shown in figure 12 for the same inlet gap but with the initial plenum volume. It can be seen from this comparison that no essential difference in flow characteristics occurs at this volume reduction, although the peak pressures tend to be somewhat higher at 5 Hz. Further sections of the flow tube totaling 279.4 cm (110 in.) were removed, and this removal resulted in a fan outlet-to-damper distance of 108.27 cm (42.63 in.) and reduced the initial plenum volume by 72 percent. The results shown in figure 17 again display much the same characteristics shown in figure 12 (initial plenum volume) and figure 16 (16-percent volume reduction) with a very slight increase in peak pressure over those in figure 16.

In the final test of this series, all sections of the flow tube were removed, and the section containing the damper (fig. 2(d)) was coupled directly to the fan. This arrangement

gave a fan outlet-to-damper distance of 16.84 cm (6.63 in.) which is a reduction of 96 percent of initial flow tube volume, and the results presented in figure 18 show substantially altered flow characteristics from any of the preceding conditions. In all cases, the "hysteresis" loop between stall and unstall is exaggerated, and peak pressures are uniformly higher, particularly at 5 Hz (fig. 18(d)). Whether such a drastic reduction in plenum volume actually alters the fan flow characteristics to this degree, or whether the extreme turbulence created by the damper operating in such proximity to the fan caused erroneous fan outlet pressure readings are matters for conjecture. There was some evidence that these are true flow characteristics since a regular cyclic variation of outlet pressure occurred for each cycle recorded. This regularity seems to discount the possibility of erroneous readings. In practical application, most air cushion landing systems have a significant "dead volume" due to ducting or trunk configurations, so that except for extreme cases it can be concluded that reductions in plenum volume have no major effect on dynamic flow characteristics.

Effects of higher damper frequencies.- The results of the preceding sections have shown significant changes in the fan flow characteristic with increasing damper frequency. In spite of these differences, however, the fan inlet and outlet pressures (from which fan flow was derived) bear a recognizable similarity to steady-state pressures as shown in figure 19 for a damper frequency of 5 Hz. To observe the effects of damper frequencies higher than 5 Hz, the fan test bench was restored to the original configuration shown in figure 1, except that the orifice was removed, and limited tests were conducted at damper frequencies of 10 Hz and 17 Hz. The resulting fan inlet and outlet pressures are shown in figure 20 for one typical cycle of damper position. It can be seen from the figure that there is no similarity to the steady-state condition and that no meaningful flow data could be derived from these erratic pressure measurements. It may be that flow transients occur at the higher damper frequencies which act to produce a momentary reverse flow through the fan. Limited tests conducted at the end of this program showed that the fan instrumentation, with the pressure taps located as shown in figure 4, was completely insensitive to flow direction through the fan. Since reverse fan flow has been observed during experimental model ACLS tests (as in ref. 1), further work is needed in this area, with the test apparatus modified to produce a reverse flow and the fan instrumentation modified to measure flow in both directions reliably.

ANALYTICAL FAN MODEL

General

Most of the analytical studies of an air cushion landing system have included realistic steady-state characteristics for the air supply fan, thus, system behavior was

predicted fairly accurately in the static mode. However, in the dynamic case, fan modeling has generally taken one of three approaches:

(1) The static characteristics have been assumed to hold good in the dynamic situation.

(2) An arbitrary time constant has been included to generate dynamic characteristics which resemble experimentally observed behavior of the total ACLS system (ref. 6).

(3) A static stable characteristic and a static stall characteristic have been determined, and in dynamic simulation an instantaneous transfer from the stable to the stall characteristic has been assumed when certain flow or pressure limits are reached (ref. 3).

Although some of these models have given a good approximation in predicting dynamic behavior, they are restricted in generality. Therefore, a need exists to develop a more general fan model which can predict the dynamic performance of a variety of ACLS fans. A key requirement of such a model is simplicity since the fan model is to be incorporated in the overall ACLS dynamic simulation. Since the natural frequencies associated with an ACLS are low (3 to 4 Hz for a model in ref. 3), initial fan model validity up to about 5 Hz is thought to be adequate.

Model Development

The model developed in this section is a generic low-frequency model for an ACLS axial-flow fan. Although the model has been developed specifically on the basis of the fan used in the experimental program, the basic characteristics cover a variety of other fans of interest for ACLS applications. In any flow region, from free flow, to stall, to zero flow and return, the actual fluid flow through the fan is quite complex. For the purpose of developing a low-frequency model, the simplified path for the fluid streamline shown in figure 4 is assumed. In the dynamic case, the inertia of the fluid particles in the fan and the capacitance of the volume inside the fan become important. The inertia of the fluid particles can be modeled by considering the flow to be composed of a number of thin stream tubes similar to the one shown in figure 4. From reference 7, the inertance of each tube is given by

$$I_{fi} = \frac{\rho l_i}{A_i} \tag{2}$$

where

I_{fi} inertance of fluid in ith stream tube

l_i flow path length for ith stream tube

ρ mean density of fluid in stream tube (air mass density)

A_i cross-sectional area of ith stream tube

If the density of the fluid in each stream tube is the same, and the flow paths are of equal length, all the inertances can be added in parallel to give

$$I_f = \frac{\rho l}{A} \tag{3}$$

where

I_f lumped inertia of fluid in fan

l average flow path length

A cross-sectional area of flow

ρ fluid density (air mass density)

A simplified lumped parameter analysis shows that the capacitance C_f of the fan is given by

$$C_f = \frac{V}{np} \tag{4}$$

where

C_f capacitance of fan

V volume of fan cavity

n polytropic constant (assumed to be 1.4)

p average air pressure (absolute) in fan

Sketch (b) shows a physical model of the fan, which describes the dynamic model in terms of physical representations of the different parameters.

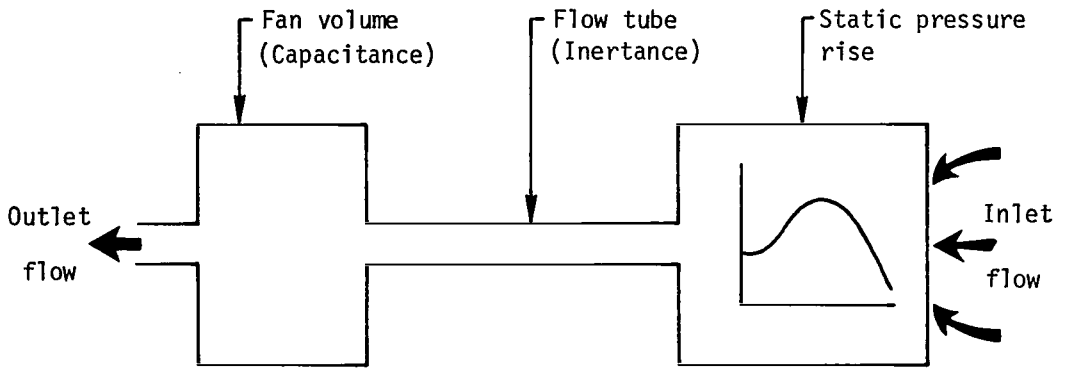

Sketch (b)

In sketch (b), the static pressure rise is shown by a steady-state characteristic curve (as shown in fig. 7, for example). A flow tube represents the inertance I_f and a volume represents the capacitance C_f. It should be recognized that the capacitance and inertance evaluated by equations (3) and (4) are lumped parameter values. For a more detailed representation of the fluid interaction, a model which distributes the inertance and capacitance over the entire stream tube can be used (ref. 8). However, for the low-frequency application of interest here, the lumped parameter model should be adequate. The analytical model of the fan thus is as shown in sketch (c).

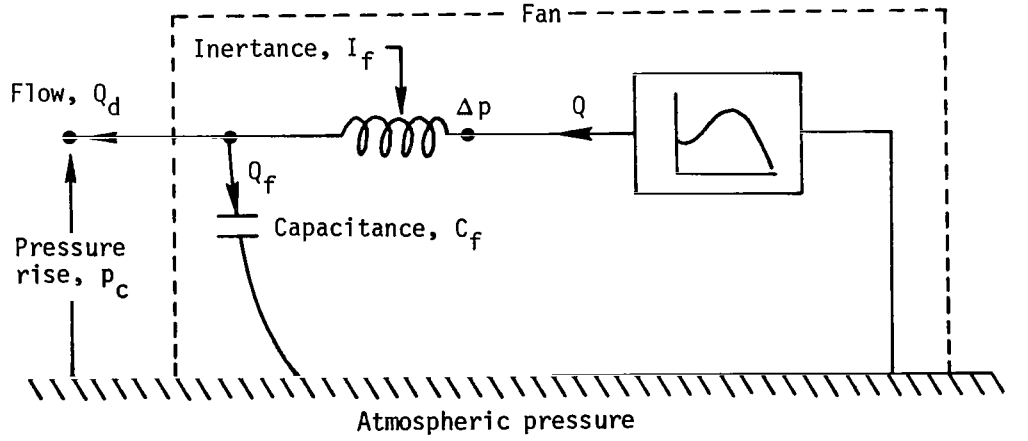

Sketch (c)

Sketch (c) represents the dynamic model in terms of equivalent electrical components for inertance and capacitance. The fan discharge or outlet pressure p_c and the fan outlet flow Q_d shown in sketch (c) can be evaluated from the following equations:

$$\frac{dQ}{dt} = \frac{\Delta p - p_c}{I_f} \tag{5}$$

$$\frac{dp_c}{dt} = \frac{Q_f}{C_f} \tag{6}$$

$$Q_d = Q - Q_f \tag{7}$$

$$\Delta p = f(Q) \text{ (steady-state characteristic)} \tag{8}$$

where

Q steady-state fan flow

Δp fan static pressure rise

Q_f capacitance flow

Q_d fan outlet flow

p_c fan outlet pressure

Equations (5) to (8) can be solved for the five unknowns Δp, p_c, Q, Q_f, and Q_d to give a dynamic relation between p_c and Q_d.

Development of Specific Test Simulation

To determine the validity of the analytical fan model, it was thought desirable to compare predicted fan behavior directly with the dynamic experimental results. Before this comparison can be accomplished, however, it is necessary that the simulation include the rotating damper and the duct between the fan and damper. The exit area controlled by the rotating damper is expressed as a variable orifice with the following relations:

$$Q_d = A_e C_e \sqrt{\frac{2p_t}{\rho}} \tag{9}$$

$$A_e = \frac{\pi D^2}{4}\left(1 - \left|\sin 2\pi ft\right|\right) \tag{10}$$

where

A_e effective exit area

C_e discharge coefficient (assumed = 0.8)

f frequency of damper shaft rotation

t time

D damper diameter (flow tube diameter)

p_t pitot static pressure upstream of damper

It should be recalled that 1 cycle of back pressure is defined as damper fully open, to fully closed, to fully open. Therefore, 2 cycles in back pressure occur per each full shaft rotation; thus, the term f in equation (10) represents a frequency half that at which the flow was varied. As previously stated, there was scant daylight clearance around the damper when fully closed. It is, therefore, assumed that because of leakage, the exit area cannot be less than 0.1 percent of the maximum area.

The combined model of the fan, duct, and damper is shown in sketch (d).

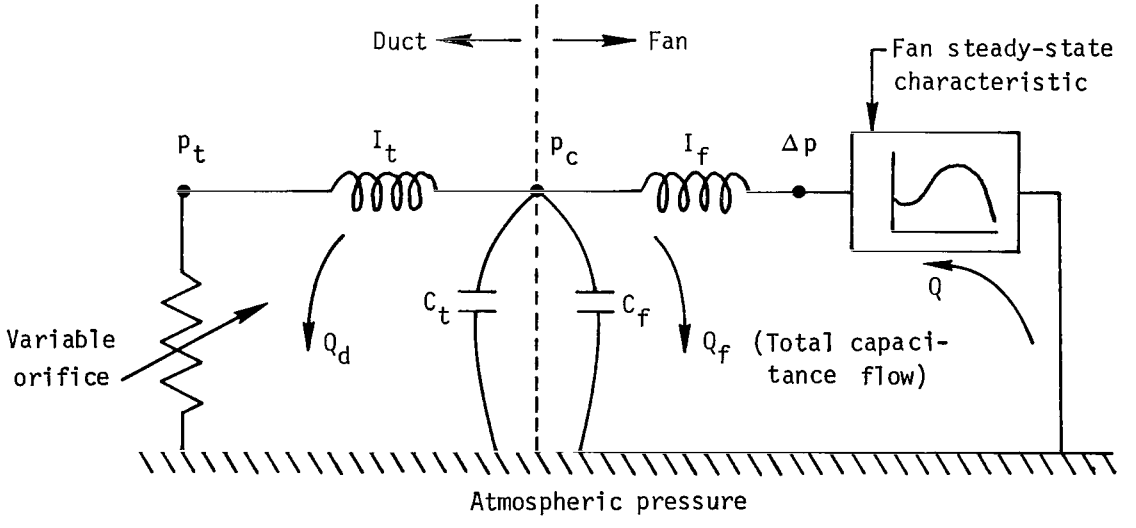

Sketch (d)

The duct between the fan and damper is modeled by a lumped capacitance C_t and a lumped inertance I_t whose magnitudes are obtained from equations (3) and (4) with the duct parameters replacing the corresponding fan parameters. In addition to the four fan model equations (eqs. (5) to (8)) and the damper area equation (eq. (10)), an equation is required to describe the outlet duct dynamics

$$\frac{dQ_d}{dt} = \frac{p_c - p_t}{I_t} \tag{11}$$

Further, the duct capacitance C_t is lumped together with the fan capacitance C_f so that equation (6) is modified with the term $C_t + C_f$ substituted for C_f in the equation. As a convenience, the equations used for the total simulation are summarized as follows:

Fan model:

$$\frac{dQ}{dt} = \frac{\Delta p - p_c}{I_f}$$

$$\frac{dp_c}{dt} = \frac{Q_f}{C_f + C_t}$$

$$Q_f = Q - Q_d$$

$\Delta p = f(Q)$ (steady-state characteristic)

Outlet duct model:

$$\frac{dQ_d}{dt} = \frac{p_c - p_t}{I_t}$$

Rotating damper model:

$$p_t = \frac{\rho}{2}\left(\frac{Q_d}{A_e C_e}\right)^2$$

For the present simulation, table III lists specific fan and duct parameters. The fan steady-state characteristic shown in figure 7 is represented by a fourth-order

polynomial in Q as follows:

$$\Delta p = \nu_0 + \nu_1 Q + \nu_2 Q^2 + \nu_3 Q^3 + \nu_4 Q^4$$

where

$\nu_0 = 65.81$

$\nu_1 = -4.902$

$\nu_2 = 1.072$

$\nu_3 = -0.03735$

$\nu_4 = 0.0003383$

Comparison With Experimental Results

The experimental results chosen for comparison with the analytical model are those presented in figure 17(a) at a damper frequency of 1.1 Hz and in figure 17(d) at a damper frequency of 5 Hz. These cases were selected since the "dead volume" between fan and damper might represent the plenum volume in an ACLS model.

The differential equations were integrated by use of a computer program incorporating a fourth-order Runge-Kutta algorithm, and the results are compared with experimental results at a damper frequency of 1.1 Hz in figure 21(a) and a frequency of 5 Hz in figure 21(b). Both analysis and experiment show that the pressure levels are higher when flow is reducing (approaching stall from free flow) than when flow is increasing (approaching free flow from stall). The difference between peak pressures for increasing flow and reducing flow is greater at 5 Hz (fig. 21(b)) than for 1.1 Hz (fig. 21(a)). One explanation for this difference is found by considering the inertance of the fluid particles in the fan I_f. By definition, dQ/dt is positive when the flow is reducing. Consequently, because of fluid inertia (eq. (5)), Δp is higher than p_c when the flow is increasing and lower than p_c when the flow is reducing. Also, the difference between p_c and Δp increases when the rate of change of Q increases, as at higher frequencies. Since Δp is a function of Q alone, and not dQ/dt, any variation in $\Delta p - p_c$ at a given Q must occur because of changes in p_c. Thus, when p_c is plotted against Q as shown in figure 21, the curves for reducing Q must lie above the curves for increasing Q with greater separation between the curves occurring for increasing frequency.

In addition to predicting the trend just discussed, the results demonstrate that the pressure levels are predicted more accurately by the dynamic model than by a model based upon static flow characteristics. Thus, the dynamic fan model developed here is capable of providing significantly improved predictions of fan behavior at back pressure frequency ranges up to 5 Hz, and, unlike previous empirical fan models, the model is quantified from physical fan parameters (length, volume, etc.) and a steady-state flow characteristic.

CONCLUDING REMARKS

This paper reports the results of an investigation of the steady-state and dynamic flow characteristics of an axial-flow fan used previously as the air supply fan in some studies of an experimental model air cushion landing system. A specially constructed fan test bench was used to determine steady-state flow characteristics using orifice differential pressure in the flow regime from free flow to zero flow. Simultaneously, fan inlet and outlet pressures were measured to develop a correlative technique so that fan pressures could be used to study dynamic flow in situations where orifice measurements cannot be used. This technique was then used to explore the effects of a variety of fan inlet and outlet conditions on fan flow characteristics at damper frequencies up to 17 Hz. Where possible, the dynamic and steady-state flow characteristics were compared to show how these differ, particularly at the higher frequencies. Based on these studies, an analytical fan model was developed which gave good correlation with experimental results. The major results of this investigation may be summarized as follows:

1. The steady-state pressure-flow characteristic curve obtained with the fan test bench agreed well with the curve provided by the fan manufacturer.

2. A relationship was established between fan inlet pressure and fan flow as measured by orifice differential pressure. Fan outlet pressure was shown to be nearly identical with upstream orifice pressure as a measure of pressure rise. These fan inlet and outlet pressure measurements were then used to study dynamic fan flow characteristics.

3. Considerable differences were shown to exist between steady-state and dynamic flow characteristics. The differences were particularly notable in the magnitude of peak pressures and in the pressure-flow relation at fan stall and unstall.

4. A restricted fan inlet was found to have a marked effect on both steady-state and dynamic flow characteristics, whereas reductions of up to 72 percent of the original plenum volume produced no significant changes in flow.

5. Dynamic flow characteristics were found to be reasonably well defined at damper frequencies up to 5 Hz, a range thought to encompass most model air cushion landing system ground operating conditions. At frequencies of 10 Hz and 17 Hz, however, fan pressures became quite erratic.

6. A need for further studies was indicated, with the test apparatus and instrumentation modified to produce and measure reverse flow, particularly at higher frequencies.

7. A generalized, rational mathematical fan model based on physical fan parameters and a steady-state flow characteristic was shown to give good agreement with experimental results at frequencies up to 5 Hz.

Langley Research Center
National Aeronautics and Space Administration
Hampton, VA 23665
April 21, 1977

REFERENCES

1. Saha, Hrishikesh, compiler: Air Cushion Landing Systems. Univ. of Tennessee Space Inst., c.1973.

2. Leland, Trafford J. W.; and Thompson, William C.: Landing-Impact Studies of a 0.3-Scale Model Air Cushion Landing System for a Navy Fighter Airplane. NASA TN D-7875, 1975.

3. Captain, K. M.; Boghani, A. B.; and Wormley, D. N.: Dynamic Heave-Pitch Analysis of Air Cushion Landing Systems. NASA CR-2530, 1975.

4. Supplement to ASME Power Test Codes. Ch. 4, Flow Measurement, Part 5 – Measurement of Quantity of Materials. PTC 19.5;4-1959, ASME, Feb. 1959.

5. Metric Practice Guide. E-380-72, American Soc. Testing & Mater., June 1972.

6. Coles, A. V.: Air Cushion Landing System CC-115 Aircraft. AFFDL-TR-72-4, Part I, U.S. Air Force, May 1972. (Available from DDC as AD 908 559.)

7. Shearer, J. Lowen; Murphy, Arthur T.; and Richardson, Herbert H.: Introduction to System Dynamics. Addison-Wesley Pub. Co., Inc., c.1967.

8. Sweet, L. M.; Richardson, H. H.; and Wormley, D. N.: Linearized Models, Stability Criteria and Experimental Verification for Plenum Air Cushions With Compressor-Duct Interactions. FRA-ORD & D-74-40, Federal Railroad Administration, May 1974.

TABLE I.- ORIFICE SIZES AND FLOW RANGES

Orifice number	Orifice diameter		Usable flow range	
	cm	in.	m^3/s	cfm
1	16.19	6.375	0.57 to 1.18	1200 to 2500
2	15.24	6.000	0.47 to 0.94	1000 to 2000
3	12.07	4.750	0.24 to 0.47	500 to 1000
4	8.26	3.250	0.09 to 0.24	200 to 500

TABLE II.- FAN INLET RESTRICTION VALUES

Fan inlet plate gap		Inlet area		Percent open[a]
cm	in.	cm^2	in^2	
2.54	1.0	227.94	35.34	168
2.03	.8	182.34	28.27	134
1.52	.6	136.80	21.21	100
1.02	.4	91.20	14.14	67
.51	.2	45.60	7.07	34

[a]Based on internal fan inlet area, 135.67 cm^2 (21.034 in^2).

TABLE III.- FAN AND DUCT MODEL TEST PARAMETERS

Parameter	Symbol	Numerical value	
Flow cross-sectional area in fan	A	0.014 m^2	0.15 ft^2
Volume of fan cavity	V	0.0042 m^3	0.15 ft^3
Average fan air pressure (absolute)	p	101.3 kPa	2116.8 lb/ft^2
Average fan flow path length	ℓ	0.357 m	1.17 ft
Air mass density	ρ	1.206 kg/m^3	0.00234 $slug/ft^3$
Polytropic constant	n	1.4	1.4
Discharge coefficient, damper orifice	C_e	0.8	0.8
Flow tube diameter (damper diameter)	D	0.203 m	0.667 ft
Distance from fan outlet to damper		1.091 m	3.58 ft
Lumped inertia of fluid in fan	I_f	0.44 Ns^2/m^5	0.018 lb s^2/ft^5
Fan capacitance	C_f	2.9×10^{-8} m^5/N	0.00005 ft^5/lb
Lumped duct air inertance	I_t	40.59 Ns^2/m^5	0.024 lb s^2/ft^5
Lumped duct capacitance	C_t	21.9×10^{-8} m^5/N	0.00037 ft^5/lb

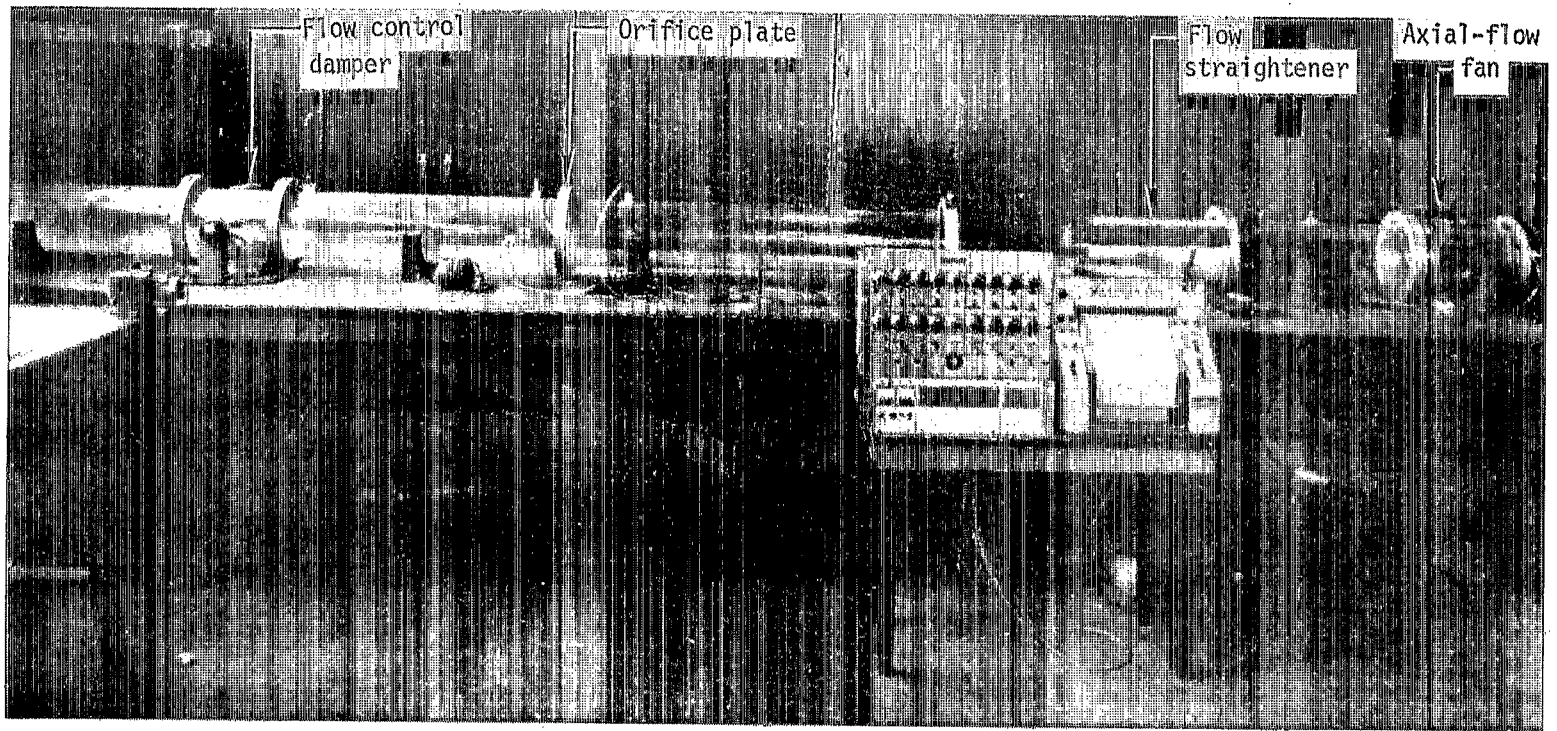

L-76-1114.1

Figure 1.- Overall view of complete fan test bench.

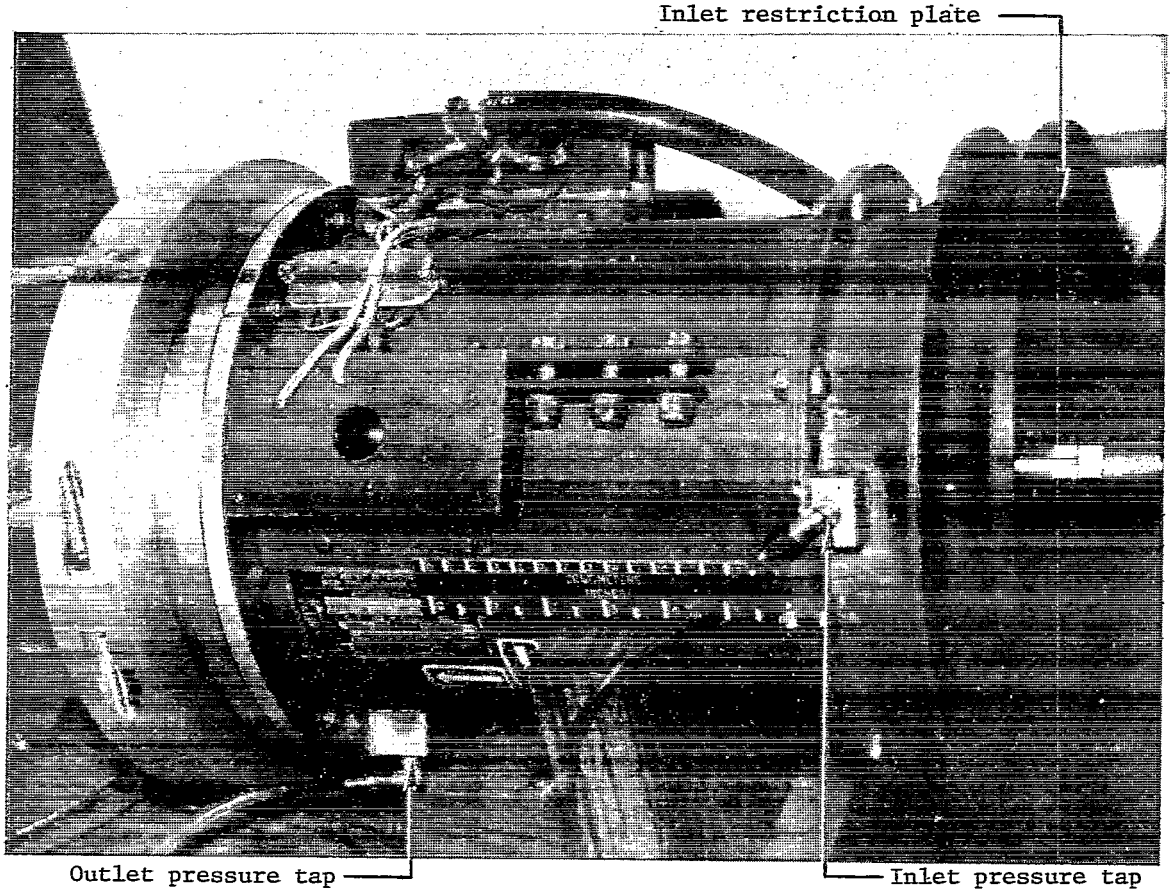

L-74-5618.1

(a) Axial-flow fan.

Figure 2.- Closeup views of key components of fan test bench.

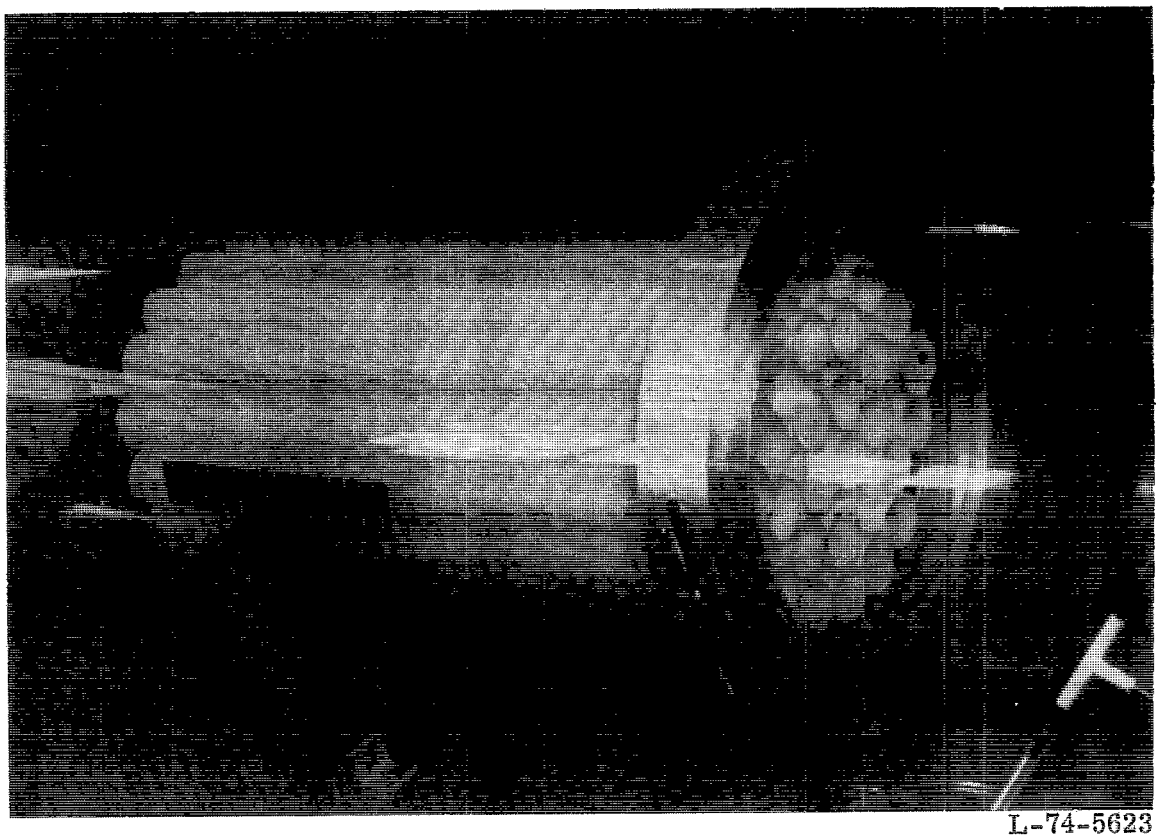

L-74-5623

(b) Flow straightener.

Figure 2.- Continued.

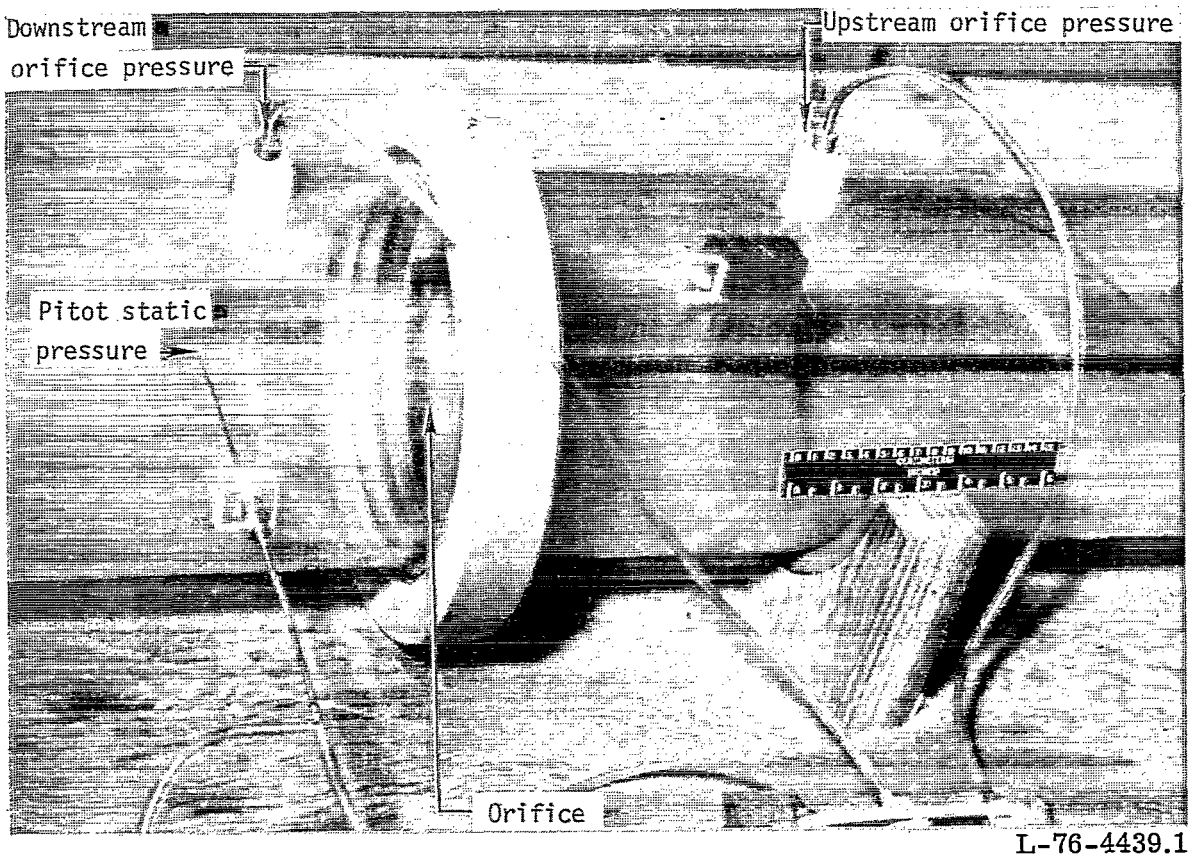

(c) Orifice plate installation.

Figure 2.- Continued.

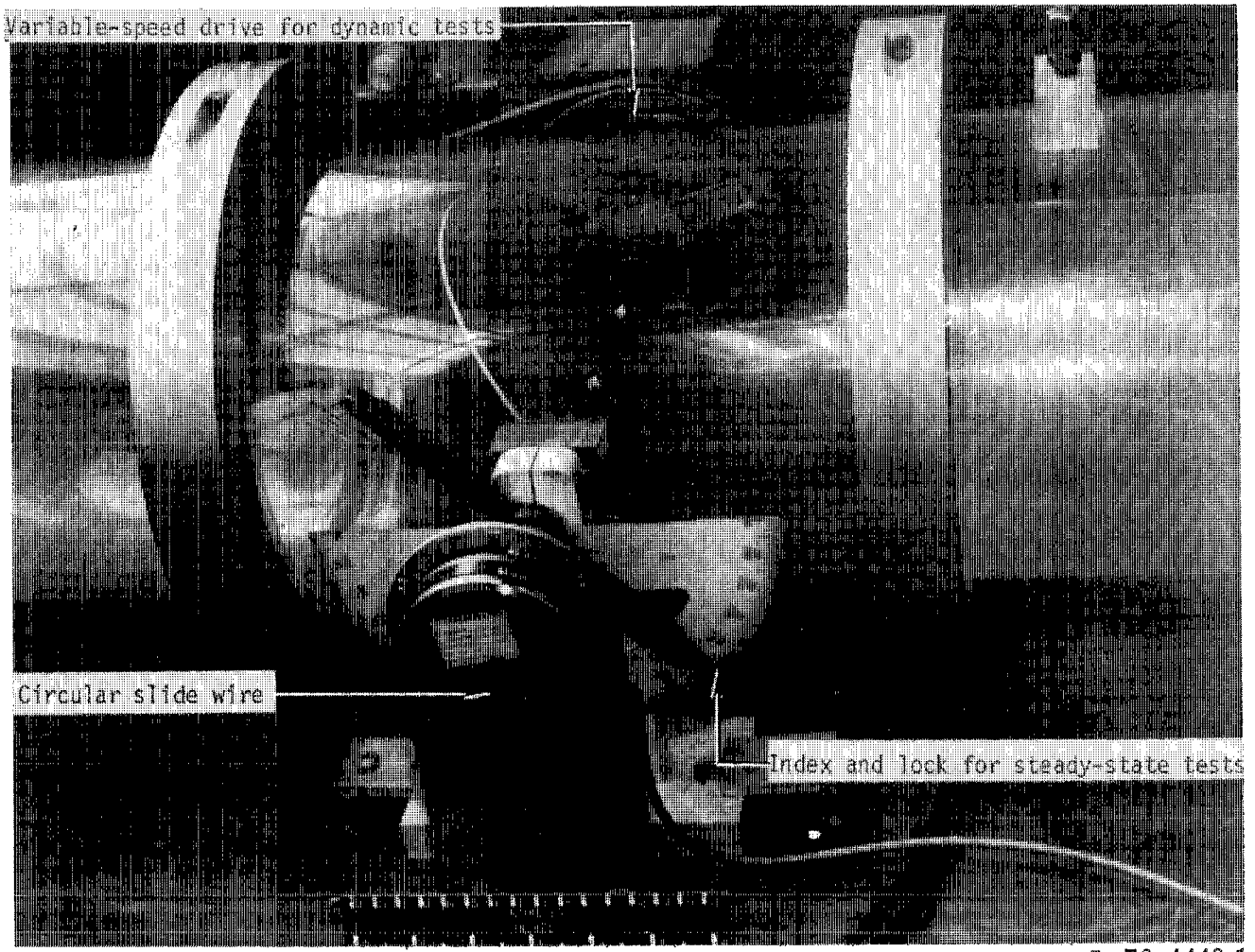

L-76-4440.1

(d) Flow control damper.

Figure 2.- Concluded.

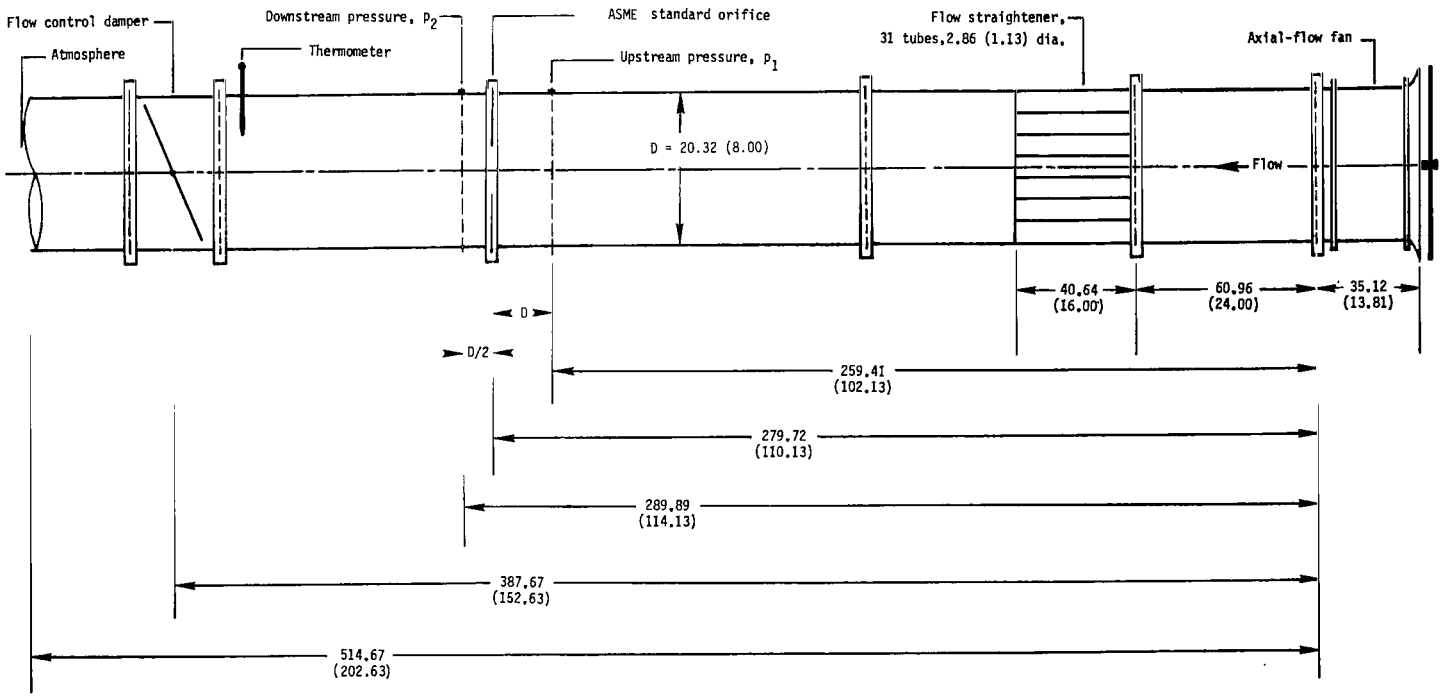

Figure 3.- Schematic of fan flow test apparatus. Dimensions are in cm (in.) and are not drawn to scale.

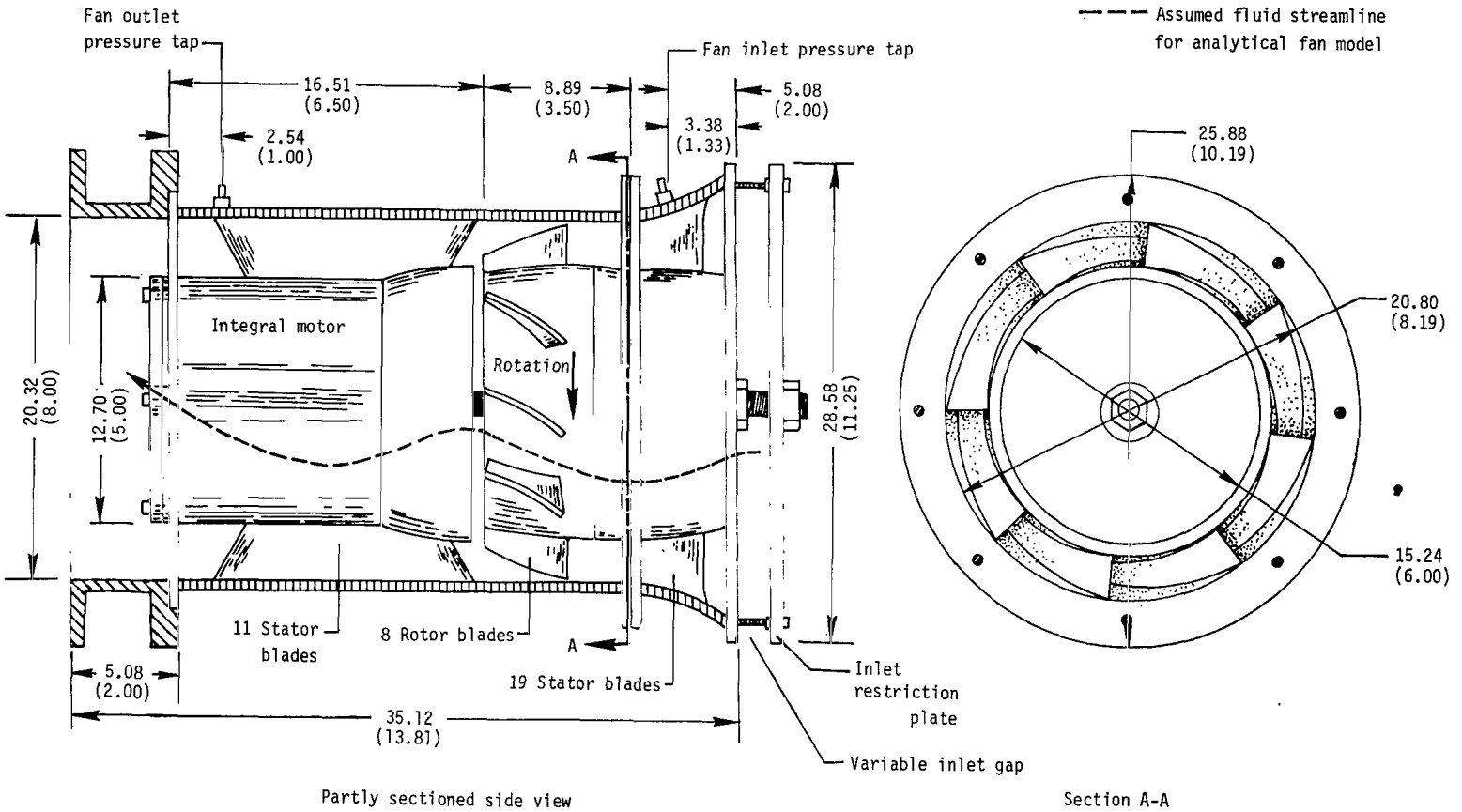

Figure 4.- Schematic of axial-flow fan used in this investigation. Dimensions are in cm (in.).

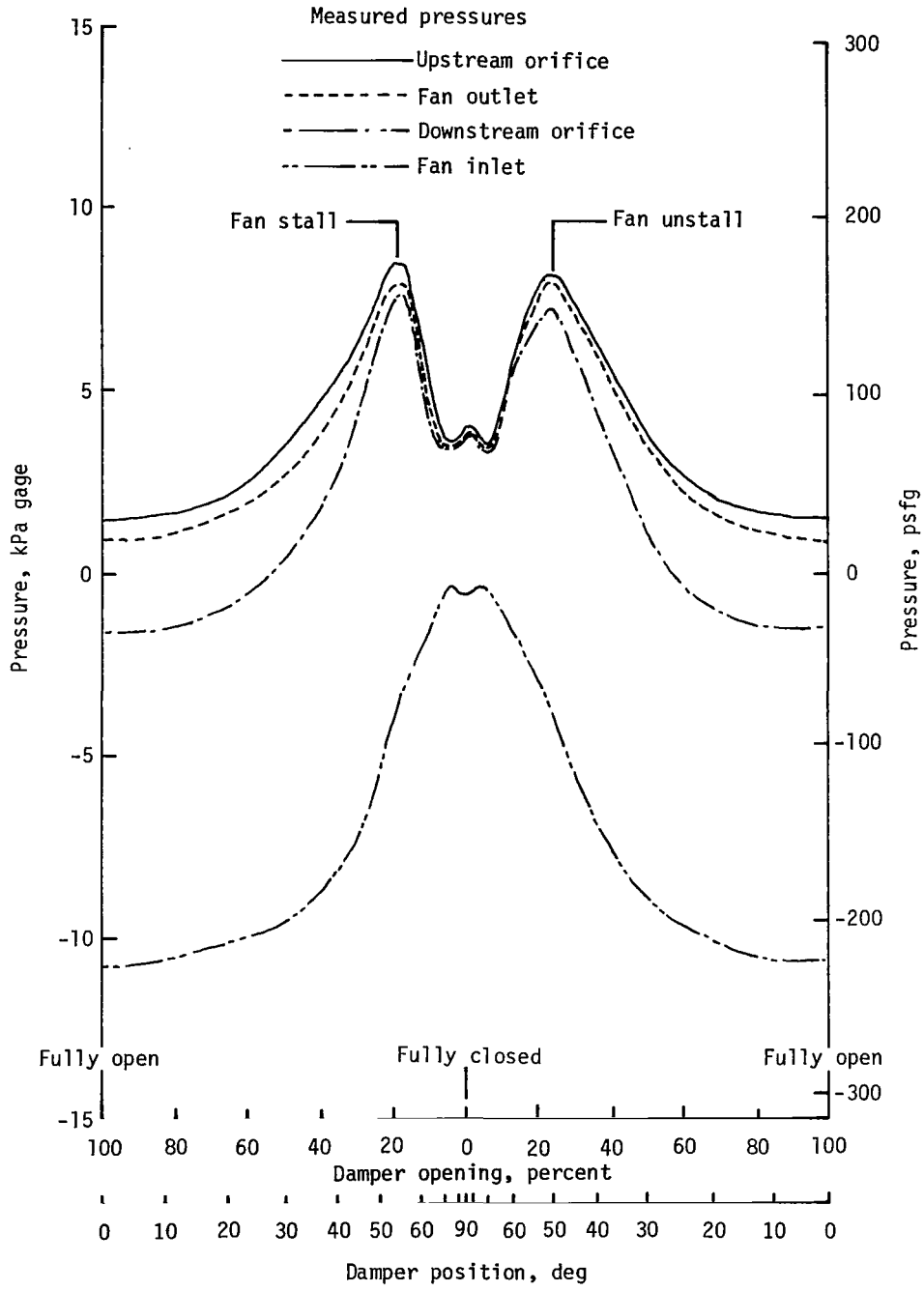

Figure 5.- Typical pressures measured during steady-state tests. Orifice number 1 (table I); inlet gap, 2.54 cm (1.0 in.).

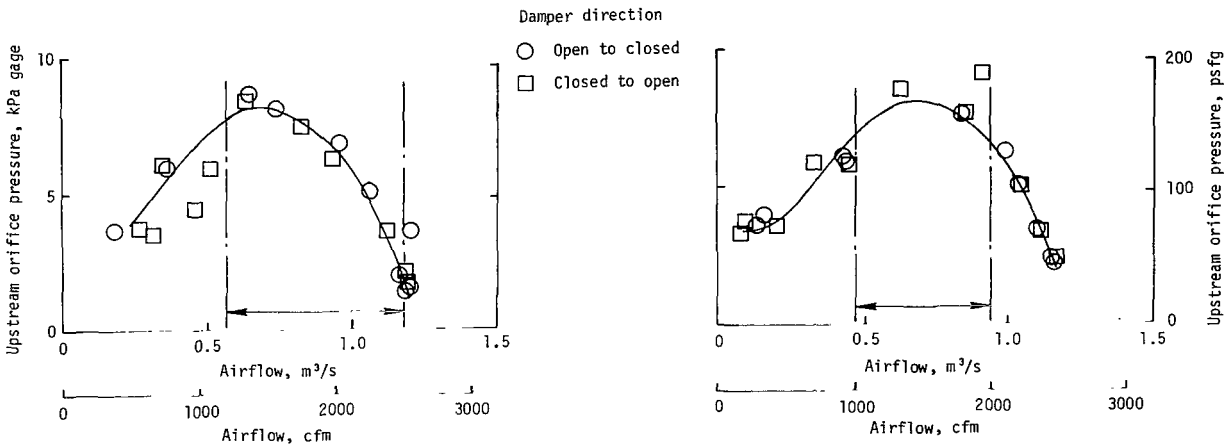

(a) Orifice number 1.

(b) Orifice number 2.

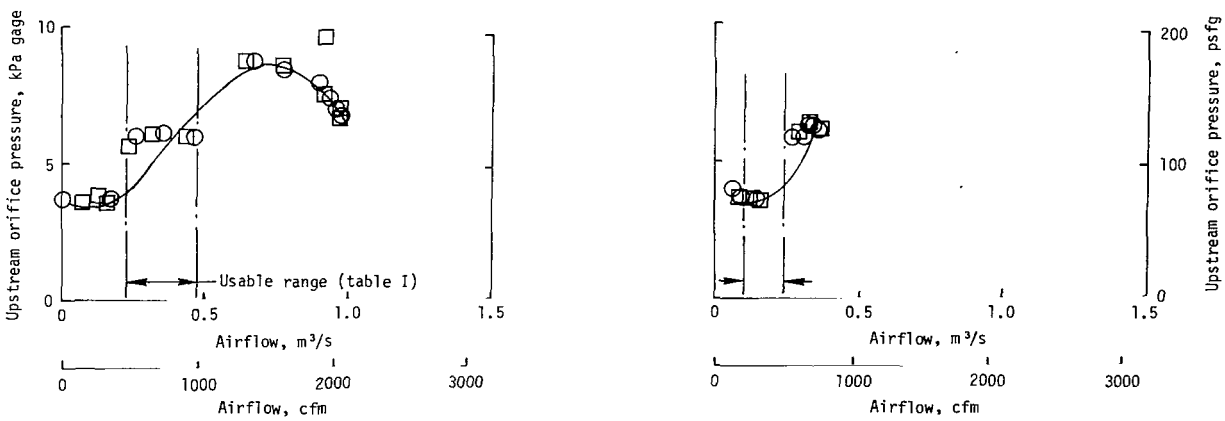

(c) Orifice number 3.

(d) Orifice number 4.

Figure 6.- Computed steady-state flow rates for four orifices. Inlet gap, 2.54 cm (1.0 in.).

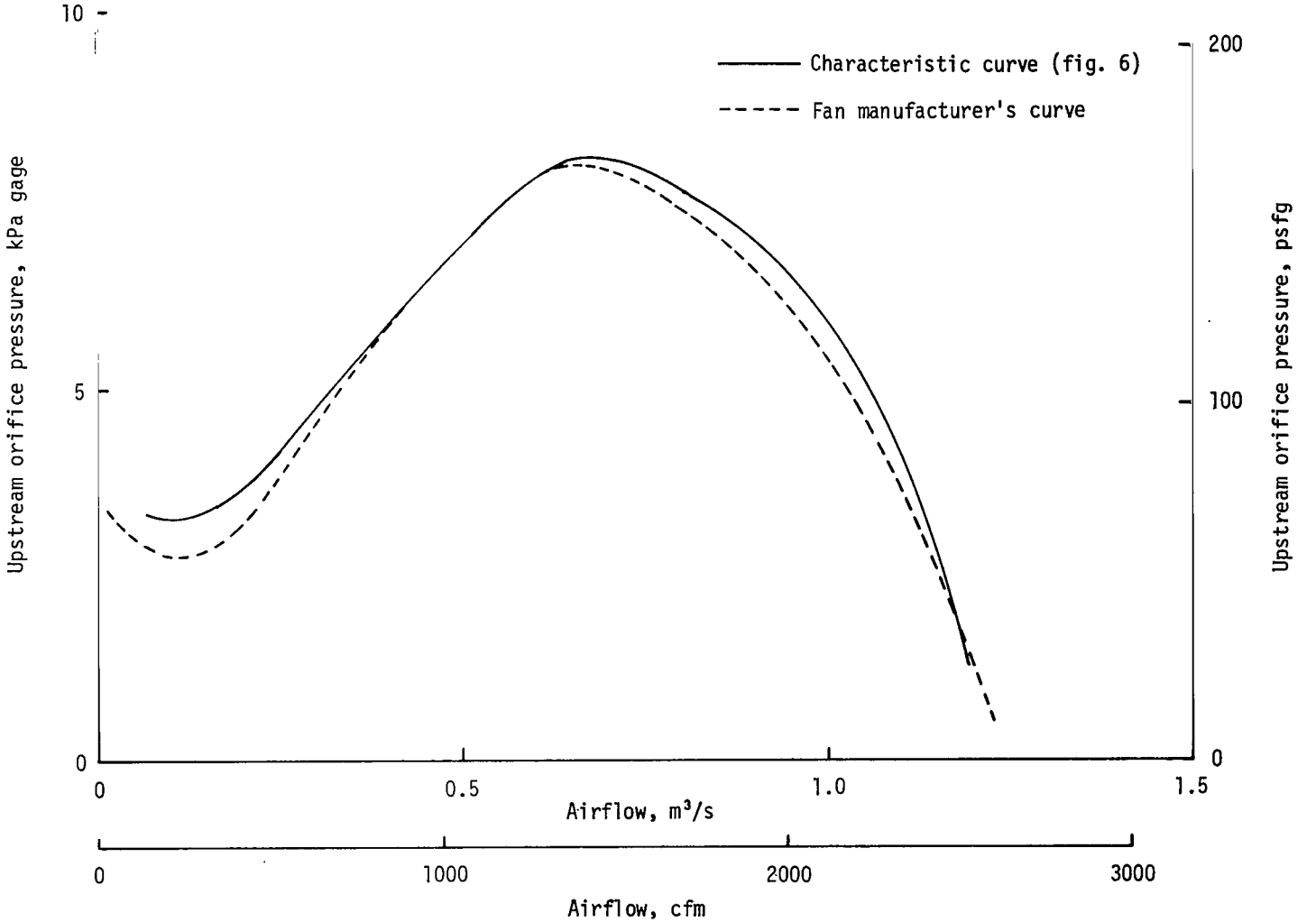

Figure 7.- Comparison of steady-state pressure-flow characteristic curve developed in this investigation with curve provided by fan manufacturer. Inlet gap, 2.54 cm (1.0 in.).

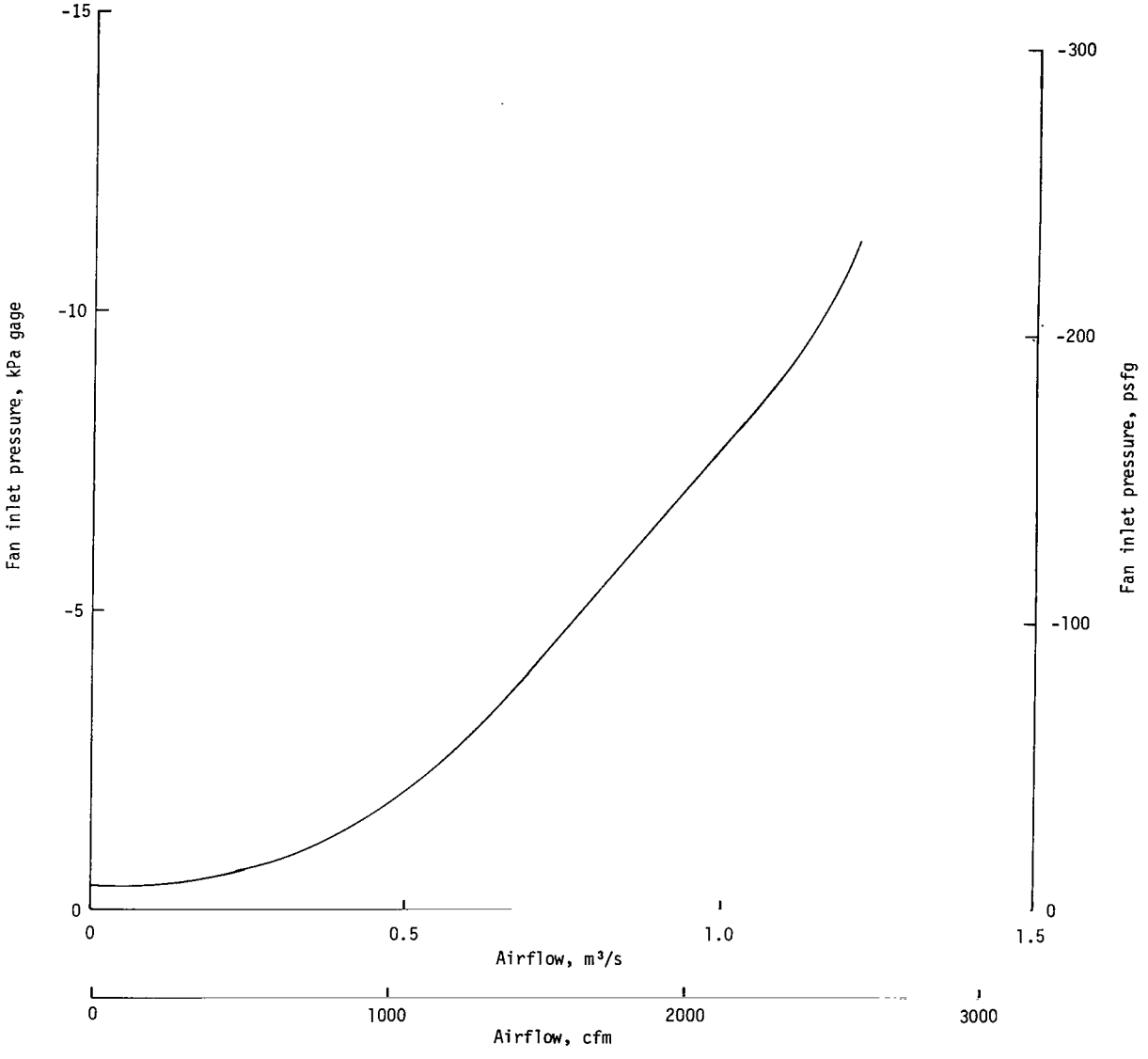

Figure 8.- Relationship of measured fan inlet pressure to airflow as computed from orifice differential pressure. Inlet gap, 2.54 cm (1.0 in.).

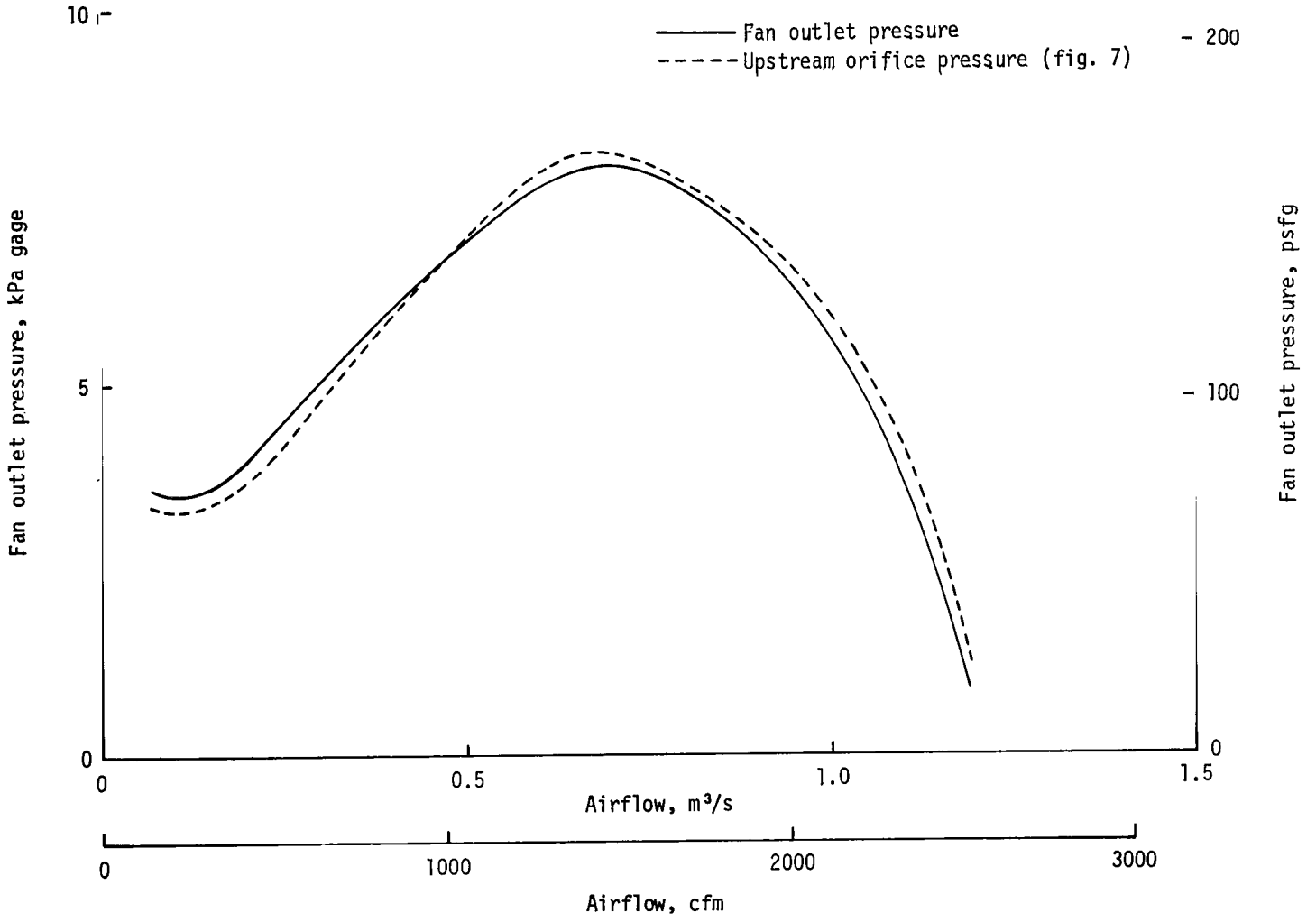

Figure 9.- Relationship of fan outlet pressure to airflow as computed from orifice differential pressure. Inlet gap, 2.54 cm (1.0 in.).

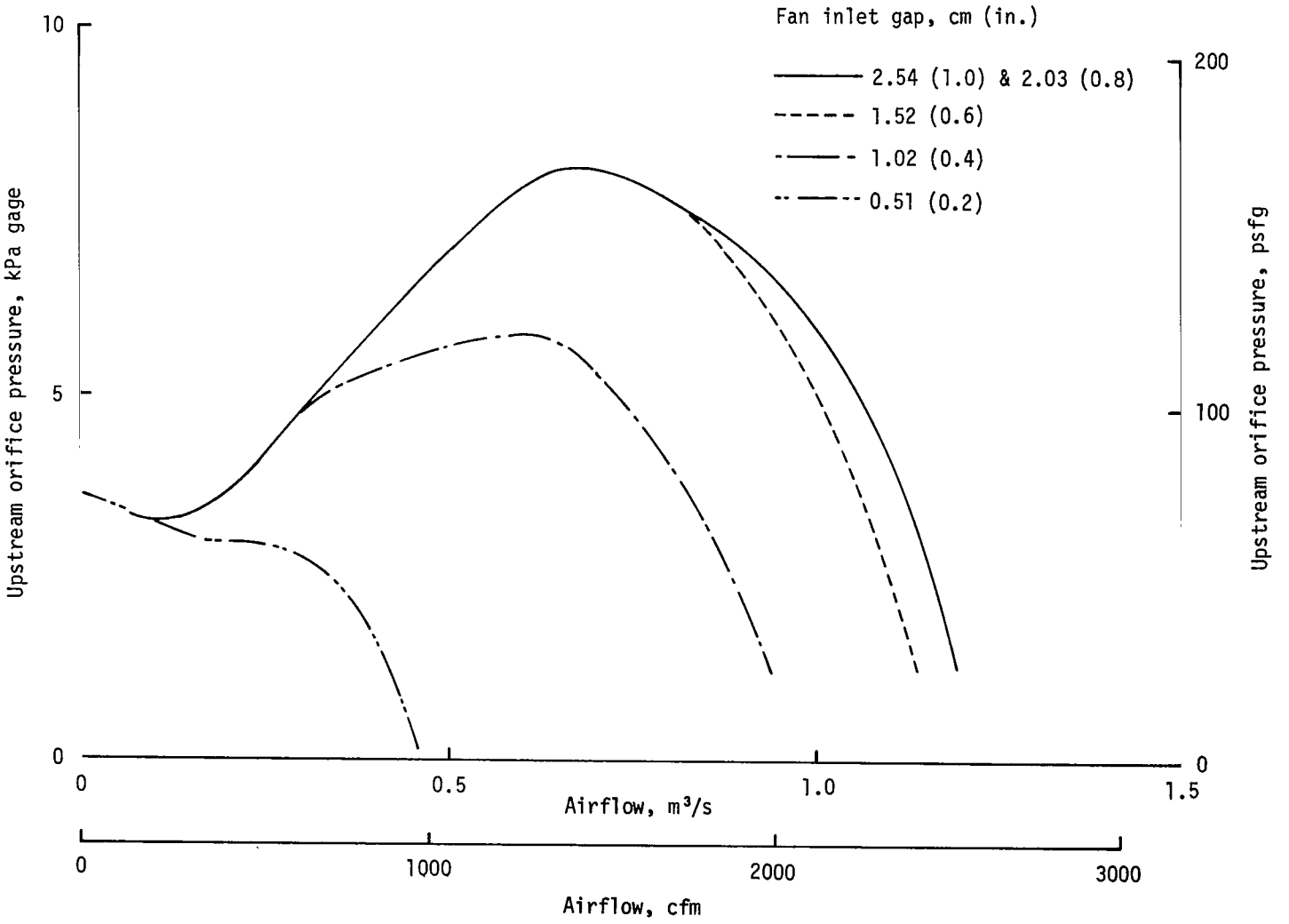

Figure 10.- Effect of fan inlet restriction on steady-state pressure-flow characteristics. Orifice sizes appropriate to flow regimes.

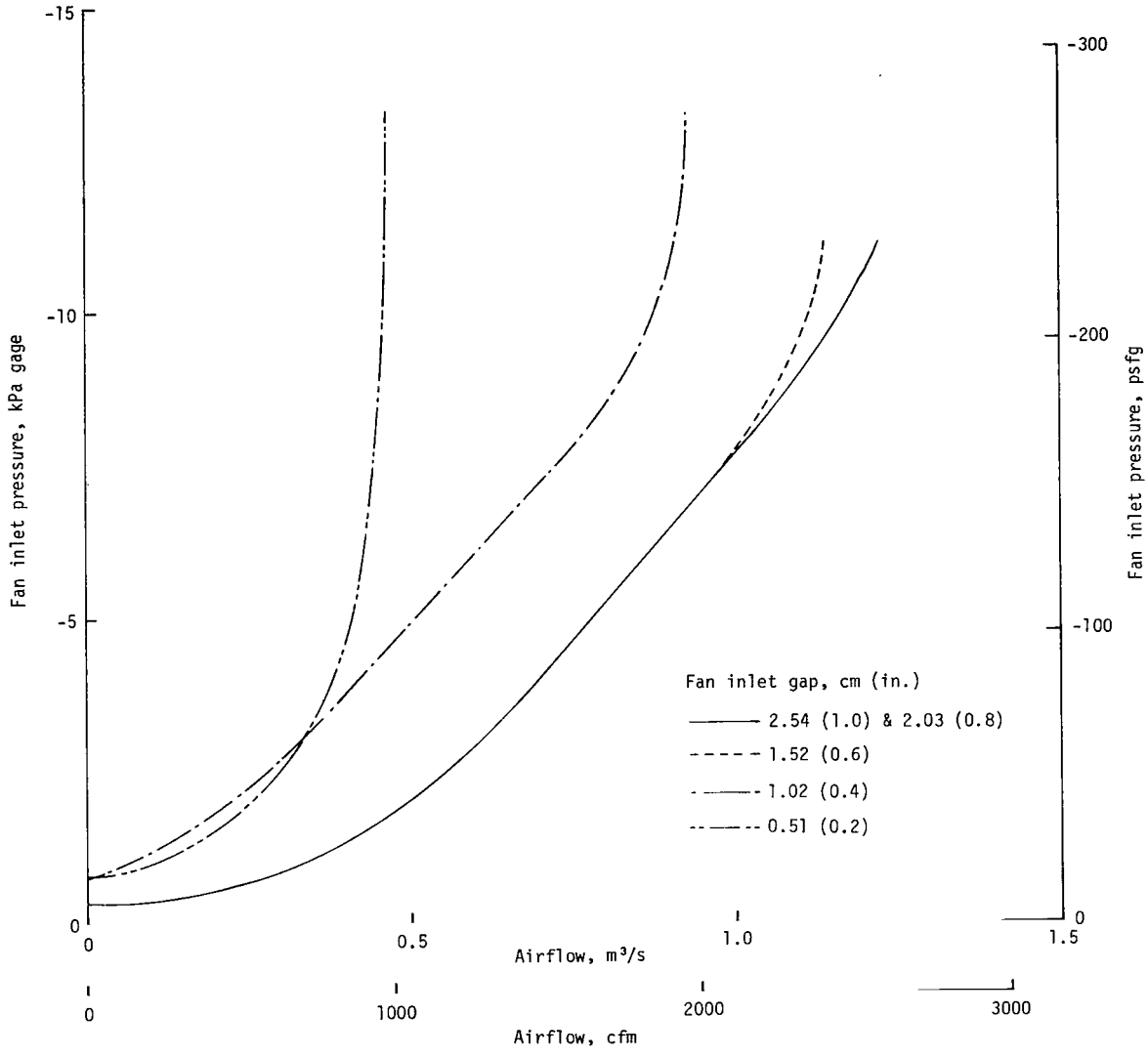

Figure 11.- Relationship of steady-state fan inlet pressure to computed airflow for range of inlet restrictions.

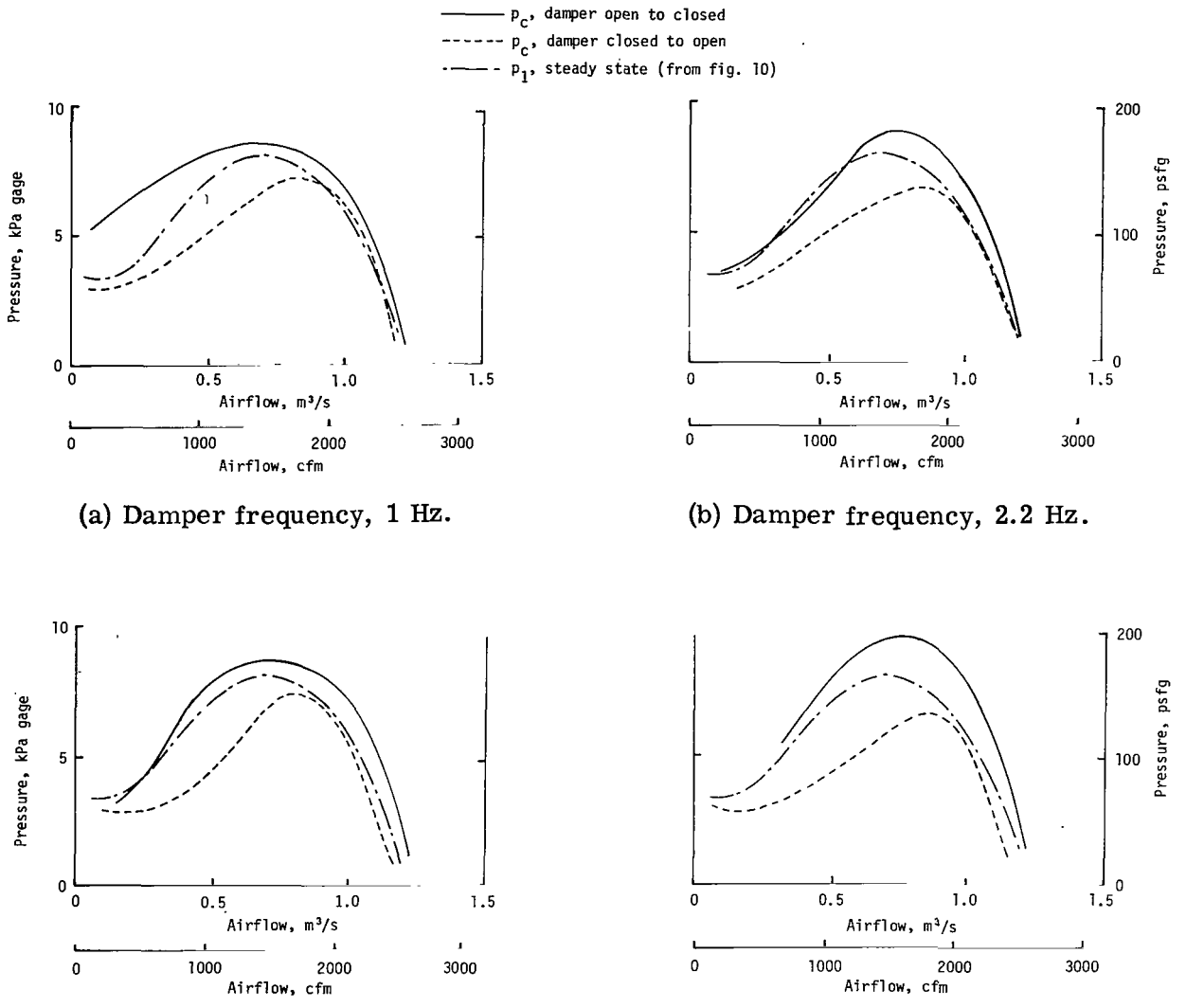

Figure 12.- Dynamic fan flow characteristics at damper frequencies up to 5 Hz; fan inlet gap, 2.54 cm (1.0 in.). Steady-state flow shown for same inlet gap.

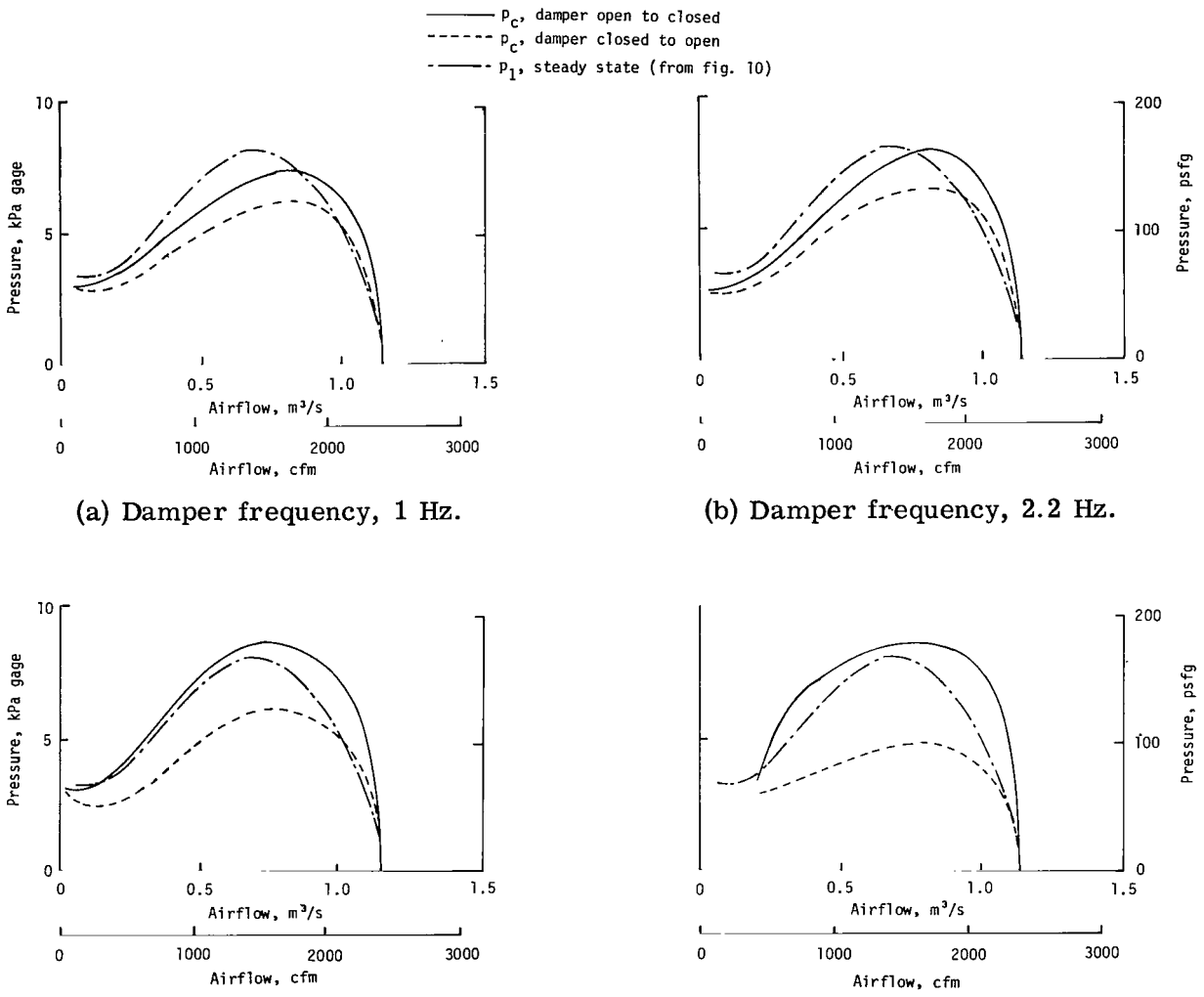

(a) Damper frequency, 1 Hz.

(b) Damper frequency, 2.2 Hz.

(c) Damper frequency, 3.3 Hz.

(d) Damper frequency, 5 Hz.

Figure 13.- Dynamic fan flow characteristics at damper frequencies up to 5 Hz; fan inlet gap, 1.52 cm (0.6 in.). Steady-state flow shown for same inlet gap.

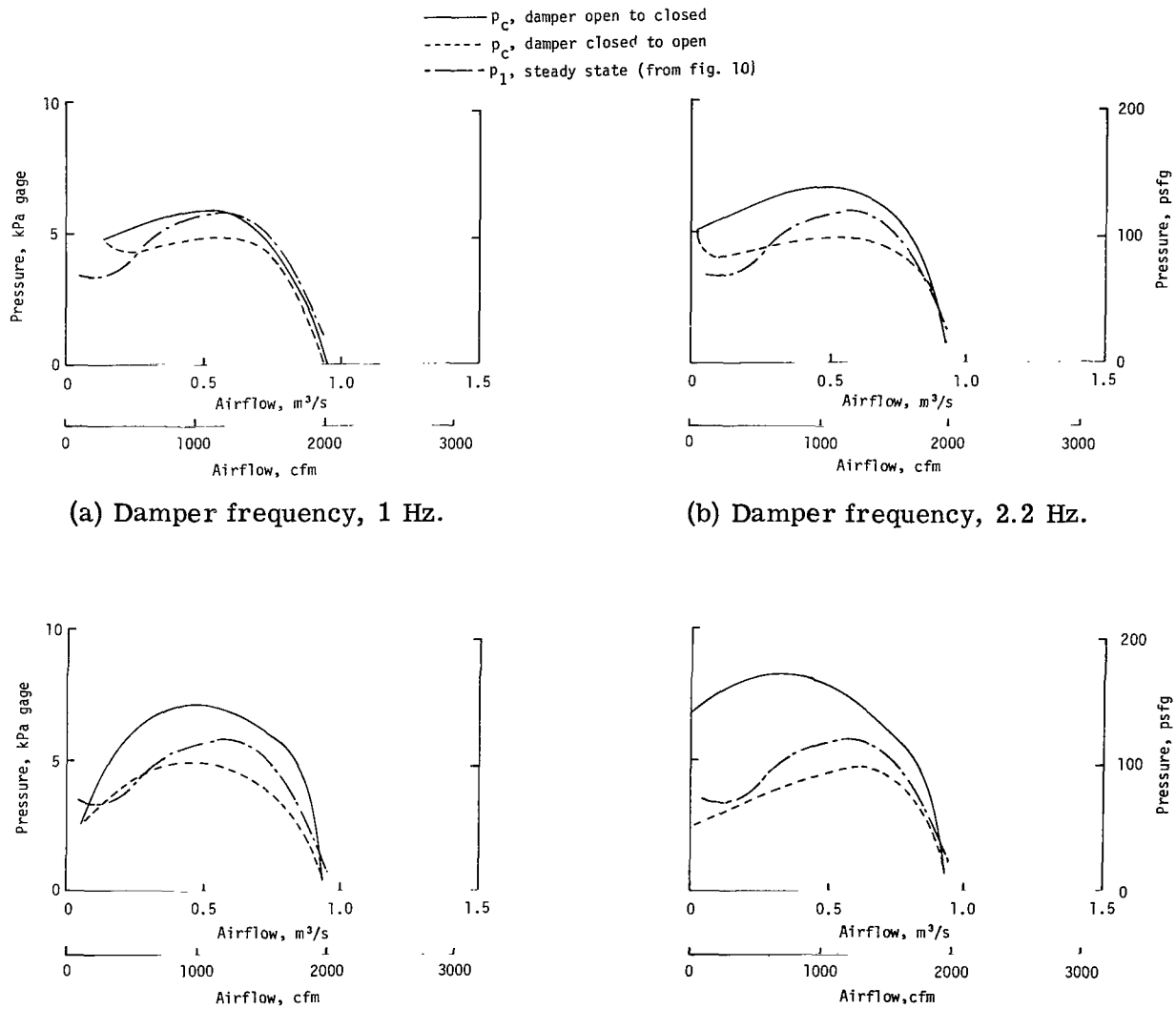

(a) Damper frequency, 1 Hz.

(b) Damper frequency, 2.2 Hz.

(c) Damper frequency, 3.3 Hz.

(d) Damper frequency, 5 Hz.

Figure 14.- Dynamic fan flow characteristics at damper frequencies up to 5 Hz; fan inlet gap, 1.02 cm (0.4 in.). Steady-state flow shown for same inlet gap.

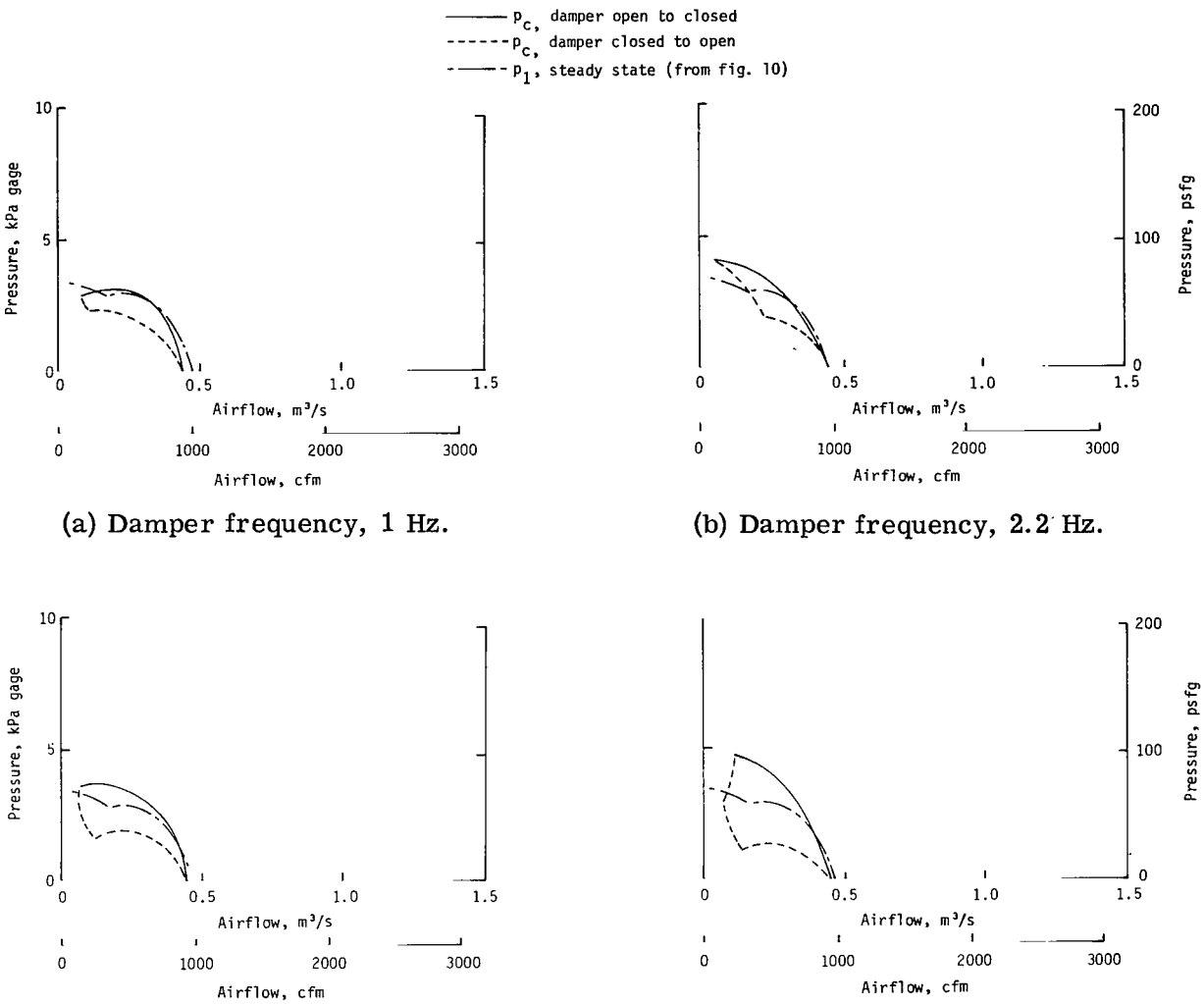

(a) Damper frequency, 1 Hz.

(b) Damper frequency, 2.2 Hz.

(c) Damper frequency, 3.3 Hz.

(d) Damper frequency, 5 Hz.

Figure 15.- Dynamic fan flow characteristics at damper frequencies up to 5 Hz; fan inlet gap, 0.51 cm (0.2 in.). Steady-state flow shown for same inlet gap.

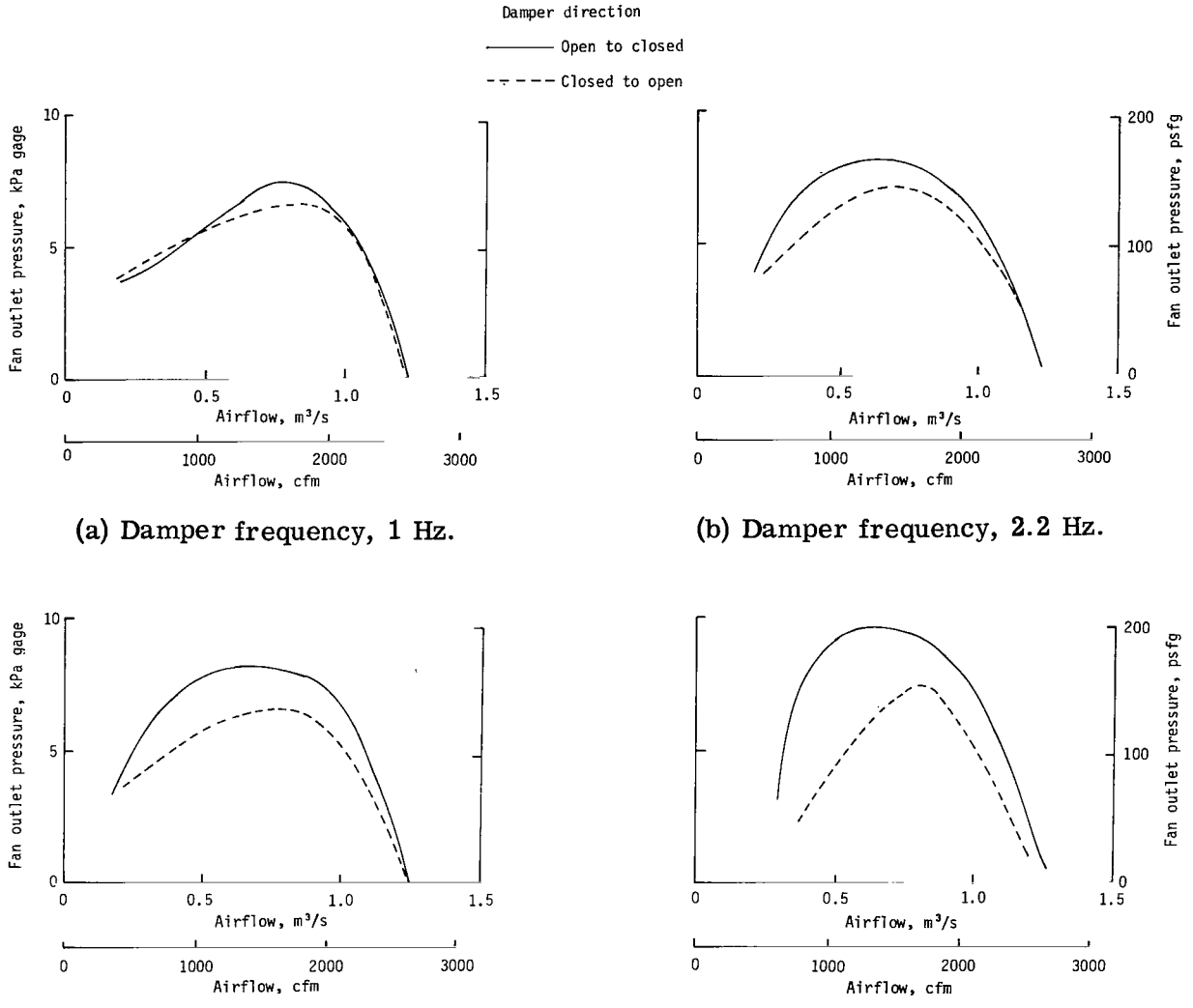

(a) Damper frequency, 1 Hz.

(b) Damper frequency, 2.2 Hz.

(c) Damper frequency, 3.3 Hz.

(d) Damper frequency, 5 Hz.

Figure 16.- Dynamic fan flow characteristics at damper frequencies up to 5 Hz; fan outlet-to damper distance, 326.67 cm (128.63 in.), a 16-percent reduction of initial plenum volume. Inlet gap, 2.54 cm (1.0 in.).

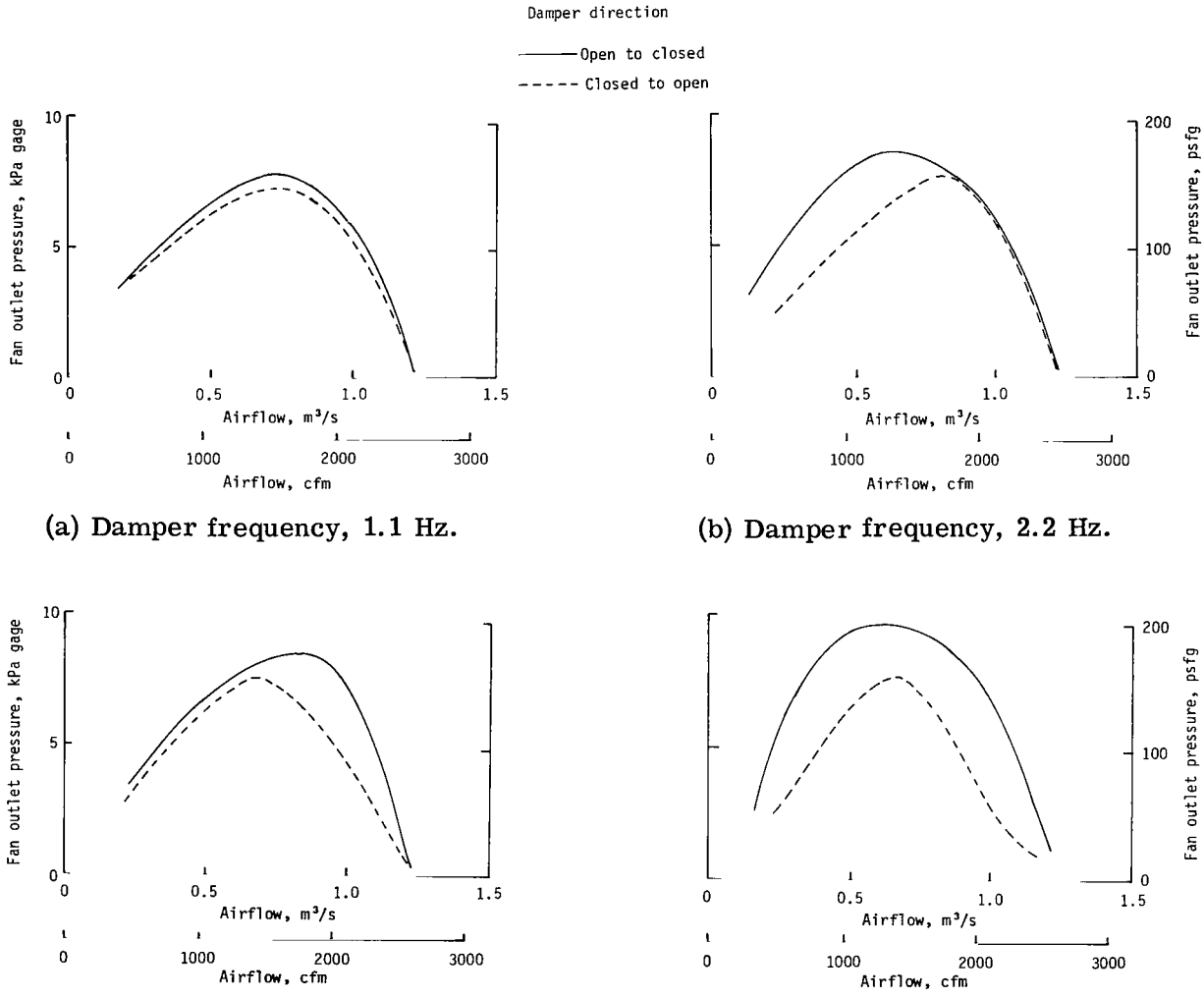

(a) Damper frequency, 1.1 Hz.

(b) Damper frequency, 2.2 Hz.

(c) Damper frequency, 3.3 Hz.

(d) Damper frequency, 5 Hz.

Figure 17.- Dynamic fan flow characteristics at damper frequencies up to 5 Hz; fan outlet-to-damper distance, 108.27 cm (42.63 in.), a 72-percent reduction of initial plenum volume. Inlet gap, 2.54 cm (1.0 in.).

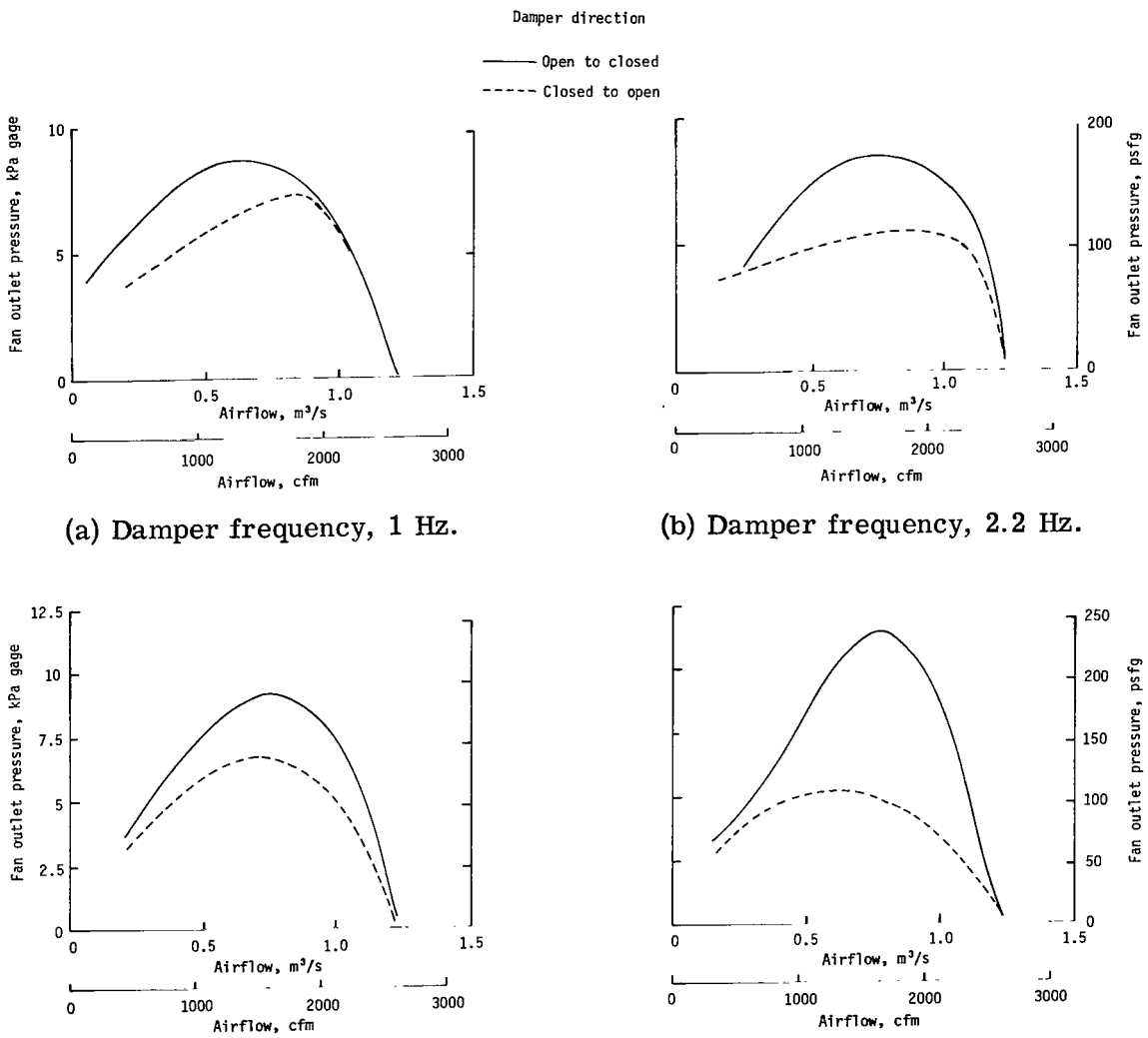

(a) Damper frequency, 1 Hz.

(b) Damper frequency, 2.2 Hz.

(c) Damper frequency, 3.3 Hz.

(d) Damper frequency, 5 Hz.

Figure 18.- Dynamic fan flow characteristics at damper frequencies up to 5 Hz; fan outlet-to-damper distance, 16.84 cm (6.63 in.), a 96-percent reduction of initial plenum volume. Inlet gap, 2.54 cm (1.0 in.).

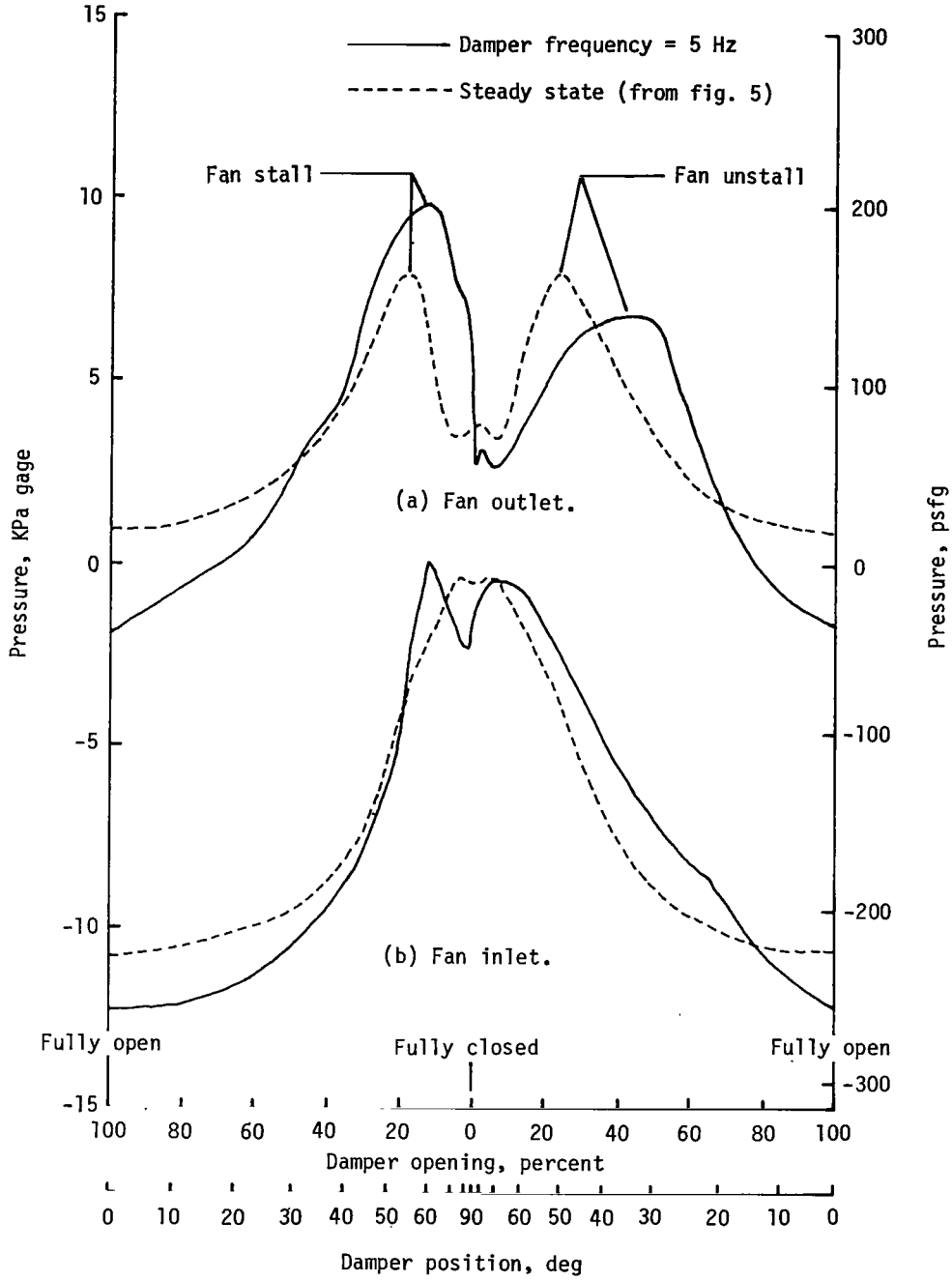

Figure 19.- Comparison of fan outlet and fan inlet pressures measured at damper frequency of 5 Hz with steady-state pressures. Fan outlet-to-damper distance, 387.67 cm (152.63 in.). Inlet gap, 2.54 cm (1.0 in.).

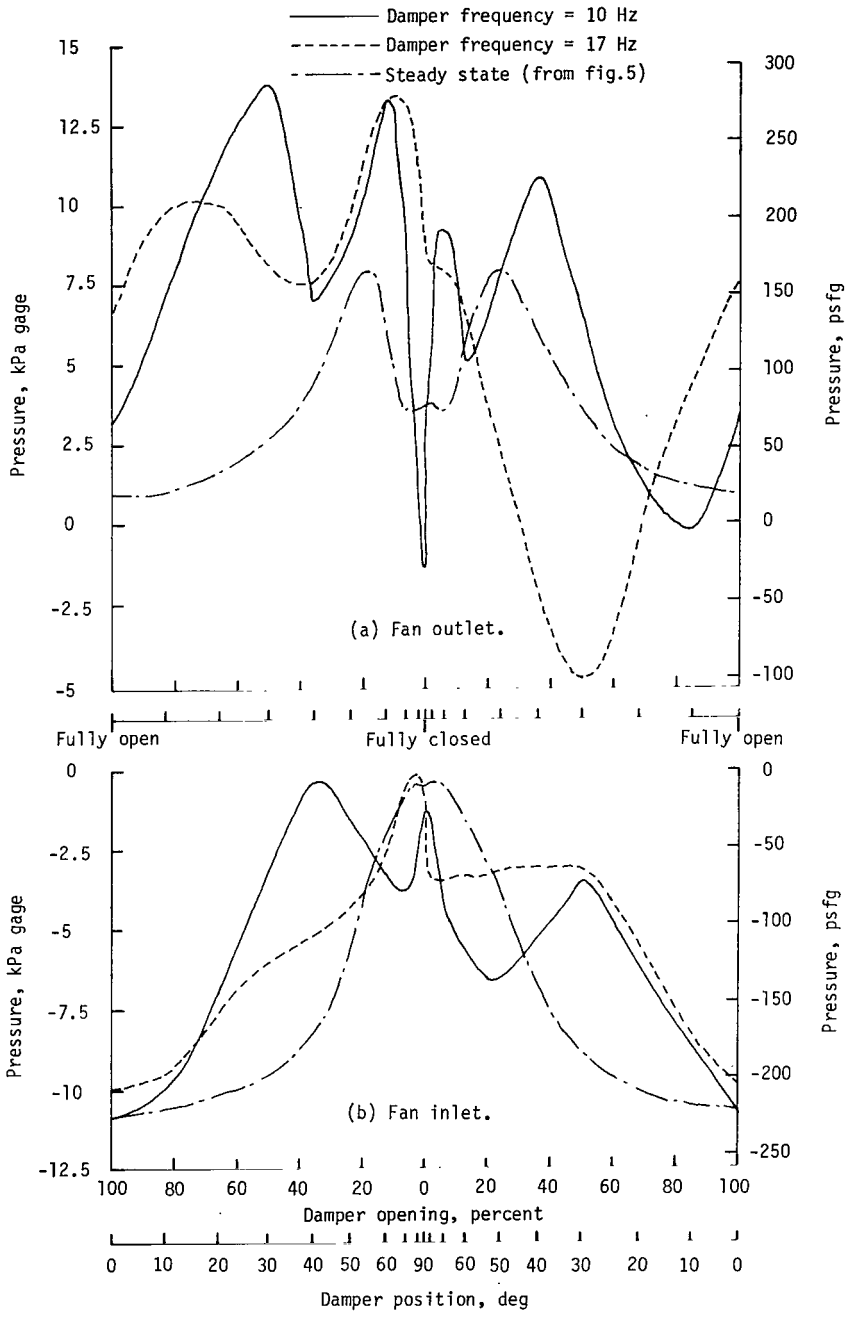

Figure 20.- Fan inlet and outlet pressures for 1 cycle at higher frequencies. Fan outlet-to-damper distance, 387.67 cm (152.63 in.). Inlet gap, 2.54 cm (1.0 in.).

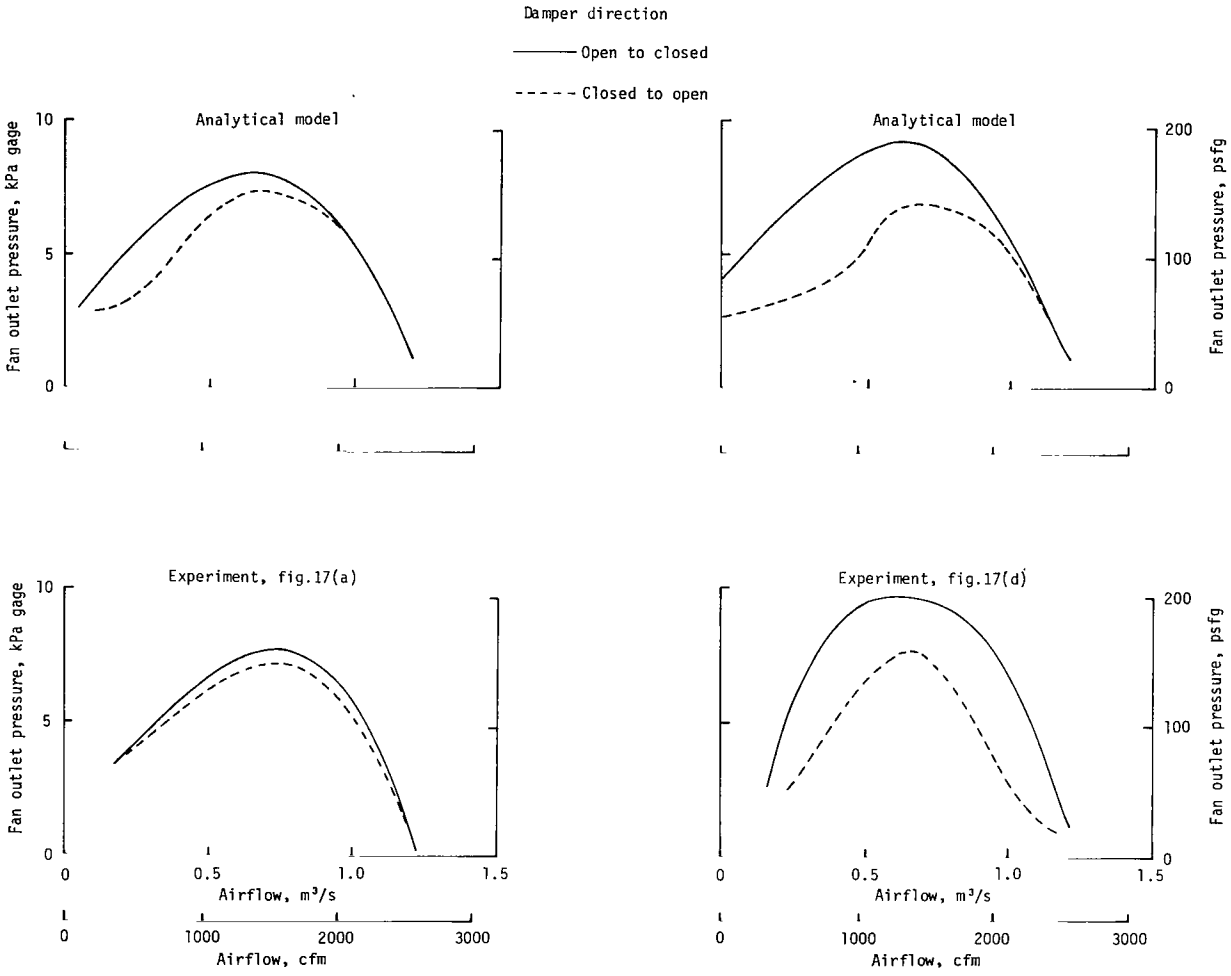

(a) Damper frequency, 1.1 Hz.

(b) Damper frequency, 5 Hz.

Figure 21.- Comparison of analytical fan model with experimental results for two damper frequencies. Fan outlet-to-damper distance, 108.27 cm (42.63 in.). Inlet gap, 2.54 cm (1.0 in.).

"The aeronautical and space activities of the United States shall be conducted so as to contribute . . . to the expansion of human knowledge of phenomena in the atmosphere and space. The Administration shall provide for the widest practicable and appropriate dissemination of information concerning its activities and the results thereof."

—NATIONAL AERONAUTICS AND SPACE ACT OF 1958

NASA SCIENTIFIC AND TECHNICAL PUBLICATIONS

TECHNICAL REPORTS: Scientific and technical information considered important, complete, and a lasting contribution to existing knowledge.

TECHNICAL NOTES: Information less broad in scope but nevertheless of importance as a contribution to existing knowledge.

TECHNICAL MEMORANDUMS: Information receiving limited distribution because of preliminary data, security classification, or other reasons. Also includes conference proceedings with either limited or unlimited distribution.

CONTRACTOR REPORTS: Scientific and technical information generated under a NASA contract or grant and considered an important contribution to existing knowledge.

TECHNICAL TRANSLATIONS: Information published in a foreign language considered to merit NASA distribution in English.

SPECIAL PUBLICATIONS: Information derived from or of value to NASA activities. Publications include final reports of major projects, monographs, data compilations, handbooks, sourcebooks, and special bibliographies.

TECHNOLOGY UTILIZATION PUBLICATIONS: Information on technology used by NASA that may be of particular interest in commercial and other non-aerospace applications. Publications include Tech Briefs, Technology Utilization Reports and Technology Surveys.

Details on the availability of these publications may be obtained from:

SCIENTIFIC AND TECHNICAL INFORMATION OFFICE

NATIONAL AERONAUTICS AND SPACE ADMINISTRATION

Washington, D.C. 20546